Science of the Total Environment 1024 (2026) 181604

Contents lists available at ScienceDirect

Science of the Total Environment

journal homepage: www.elsevier.com/locate/scitotenv

Closing the plastic budget equation in fluvial systems: A review of monitoring methods

Ana Todorova [a], Robert K. Niven [a,b], Matthias Kramer [a,*]

[a] School of Engineering and Technology (SET), The University of New South Wales, Canberra, ACT, 2610, Australia
[b] Department of Mechanical Engineering, School of Engineering, Computer and Mathematical Sciences, Auckland University of Technology, Auckland, New Zealand

HIGHLIGHTS

- Generalized budget equation for fluvial plastics based on Reynolds Transport Theorem.
- Evaluation of monitoring methods across transport layers and storage compartments.
- Identification of key knowledge gaps and priorities for future monitoring research.

GRAPHICAL ABSTRACT

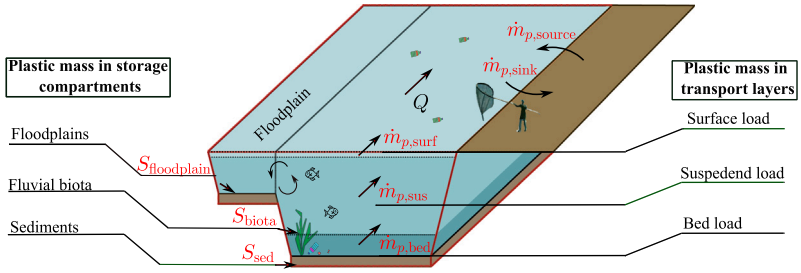

ARTICLE INFO

Keywords:
Plastic monitoring
Plastic budget equation
Direct sampling
Visual sampling

ABSTRACT

As plastic waste increasingly accumulates in aquatic environments, recent efforts have focused on quantifying the contribution of riverine sources to the ocean's plastic pollution. Accurate monitoring of fluvial plastics is challenging because plastics are transported and stored in different layers and compartments. Some processes, such as surface transport, can be measured relatively easily, while others, including bed load transport or storage in biota, remain difficult to assess. We start with a generalized formulation of the plastic budget equation, where we identify several transport and storage terms. Subsequently, we review common monitoring methods for plastics transported as surface load, suspended load, and bed load, as well as for plastics stored in sediments, floodplains, and fluvial biota. Overall, we hope to contribute to a better understanding and monitoring of fluvial plastic dynamics, with the aim to support the development of viable strategies regarding plastic pollution management and remediation.

Contents

* Corresponding author.
E-mail address: m.kramer@unsw.edu.au (M. Kramer).

https://doi.org/10.1016/j.scitotenv.2026.181604
Received 16 September 2025; Received in revised form 5 January 2026; Accepted 20 February 2026
Available online 6 March 2026

1. Introduction

After being first patented in the early 1900s, the invention of plastics has provided society a material with almost limitless possibilities. Due to its beneficial characteristics, such as being affordable, durable, lightweight, and easily moldable, the popularity of plastics drastically increased during the 20th century, while plastic production is still on the rise as of today (van Emmerik and Schwarz, 2020; Andrady and Neal, 2009; Geyer et al., 2017). Initially, plastics were mainly utilized for long-lasting products, but nowadays, a growing portion of plastic is used for single-use purposes. Plastics are highly durable and resilient, making them difficult to dispose of, with some types taking thousands – even tens of thousands – of years to degrade in landfills (Museum, 2024; Andrady, 2003). Therefore, as more plastic waste accumulates in the natural environment, it has become clear that poses significant threats to aquatic life and ecosystems (Derraik, 2002; Andrady and Neal, 2009; Gall and Thompson, 2015).

Jambeck et al. (2015) estimated that 4.8 to 12.7 million tons of plastics could be entering the marine environment from land-based sources yearly, with a prediction of a significant increase in the near future if no actions are taken. However, these estimations rely on limited field data, and they are subject to a substantial lack of knowledge on plastic transport and accumulation in different compartments, implying that significant uncertainties are present. The lack of data and knowledge on the plastic mass flow from rivers to the sea, as well as on plastic sources and sinks, hinders the implementation of appropriate environmental regulations and mitigation measures (González-Fernández and Hanke, 2017). Therefore, to effectively address plastic litter pollution on a global scale, it is crucial to quantify plastic mass flow in rivers, followed by an identification of hot spots, and a characterization of sources.

1.1. Physical parameters

The physical properties of plastics, particularly their density, type, shape, and size, play a crucial role in understanding their transport and accumulation within the transport layers and different compartments of a river system. The densities of plastics typically range from 0.85 to 1.41 kg/m^3 (Chubarenko et al., 2016), which includes positively and negatively buoyant plastics. In terms of their physical transport mechanism, positively buoyant plastics become trapped at the water's surface, while negatively buoyant plastics travel within the suspended layer and along the riverbed, thereby accumulating in riverbed sediments and floodplains. Thus, density differences dictate transport pathways and storage locations.

Plastics are commonly classified by size, and they are divided into different categories, such as microplastics (<5 mm), mesoplastics (5–25 mm), macroplastics (25 mm–1 m), and megaplastics (> 1 m) (Kershaw et al., 2019). They can be further categorized into primary plastics, which are designed for specific functions, or into secondary plastics, arising from the fragmentation or degradation of larger primary items (Barnes et al., 2009). Beyond size, the shape and surface properties of plastics significantly influence their transport behavior. For instance, thin foils and plastics with a high surface area to mass ratio are particularly susceptible to surface contamination, such as mud deposition or biofouling. These processes increase the density, reduce buoyancy, and are causing plastics to sink to the lower water column. As a result, the physical structure and environmental interactions directly affect the motion and distribution of plastics in aquatic systems (van Emmerik and Schwarz, 2020).

Previous studies have employed a variety of field techniques to assess the physical characteristics of plastics across different riverine compartments, like the water surface and column, sediments, river banks and biota (van Emmerik and Schwarz, 2020; Hurley et al., 2023). Building on these approaches, Table 1 presents a structured evaluation of various sampling and observation techniques, highlighting the physical parameters they measure and their applicability across compartments. It outlines the particle size ranges that each method can detect, and the specific physical properties of the plastics they measure. While all monitoring techniques are able to determine plastic abundance (count), polymer type, and shape, it is worth noting that only direct measurement methods can estimate plastic mass or mass flow.

1.2. Scope and outline of this review

This review aims to provide a thorough overview of the current strategies in fluvial plastic sampling/monitoring (Fig. 1). In the following sections, we will elaborate on the plastic budget equation and its significance in characterizing plastic mass associated with different transport layers and storage compartments, while accounting for localized sources and sinks (Section 2). Next, we explore the monitoring of transport layers and storage compartments, covering the water surface and column (Sections 3 and 4), riverbed and sediments (Sections 5 and 6), riverbanks and floodplains (Section 7), and fluvial biota (Section 8). For each transport layer or compartment, we assess direct and visual sampling methods, discussing their strengths, limitations, and applicability. Accordingly, Table 1 summarizes the particle-size ranges for which each sampling method is suitable, thereby delineating the reviewed methods across size classes (micro-, meso-, and macroplastics), such that general references to "plastics" throughout the manuscript should be interpreted in the context of these method-specific size constraints. Subsequently, we present a comprehensive discussion on time and length scales of the monitored plastics (Section 9.1), and on opportunities for expanding the physical parameter space (Section 9.3). Finally, we articulate the limitations of current implementations and suggest directions for future research (Section 9.4).

Table 1
Evaluation of performance of considered methods. N – count, $\triangle$ –polymer type and shape, ρ – density, m – plastic mass, $\dot{m}$ – plastic mass flow rate, A – area.

Transport layer/ Storage compartment	Measurement method	Particle size	Properties measured
Water surface & column	Nets	Micro, meso, macro	$N, \triangle, \rho, \dot{m}_{p,\text{surf}}, \dot{m}_{p,\text{sus}}$
	Bulk sampling	Micro, nano	$N, \triangle, \rho, m_{p,\text{surf}}, m_{p,\text{sus}}$
	Booms	Meso, macro	$N, \triangle, \rho, (m_{p,\text{surf}} + m_{p,\text{sus}})$[1]
	Waste collection	Meso, macro	$N, \triangle, \rho, m_{p,\text{surf}}$
	Human observation	Meso, macro	$N, \triangle$
	Standard cameras	Meso, macro	$N, \triangle$
	Spectral cameras	Micro, meso, macro	$N, \triangle, \rho$[2]
River bed & sediments	Nets	Micro, meso, macro	$N, \triangle, \rho, \dot{m}_{p,\text{bed}}$
	Physical traps	Micro, meso	$N, \triangle, \rho, \dot{m}_{p,\text{bed}}$
	Shovel	Micro, meso	$N, \triangle, \rho, \dot{m}_{p,\text{sed}}$
	Grab sampling	Micro, meso	$N, \triangle, \rho, m, m_{\text{sed}}$
	Corer sampling	Micro, meso	$N, \triangle, \rho, m, m_{\text{sed}}$
River banks & floodplains	Waste collection	Micro, meso, macro	$N, \triangle, \rho, m_{\text{floodplain}}$
	Core driving	Micro, meso	$N, \triangle, \rho, m_{\text{floodplain}}$
	Cameras	Meso, macro	$N, \triangle, m_{\text{floodplain}}$
Fluvial biota	Manual sampling	Micro, meso	$N, \triangle, m_{\text{biota}}$
	Human observers	Meso, macro	$N, \triangle, m_{\text{biota}}$
	Cameras	Meso, macro	$N, \triangle, A, m_{\text{biota}}$

[1] Booms provide bulk concentrations, which are not compartment specific.
[2] Spectral cameras are currently limited to laboratory use.

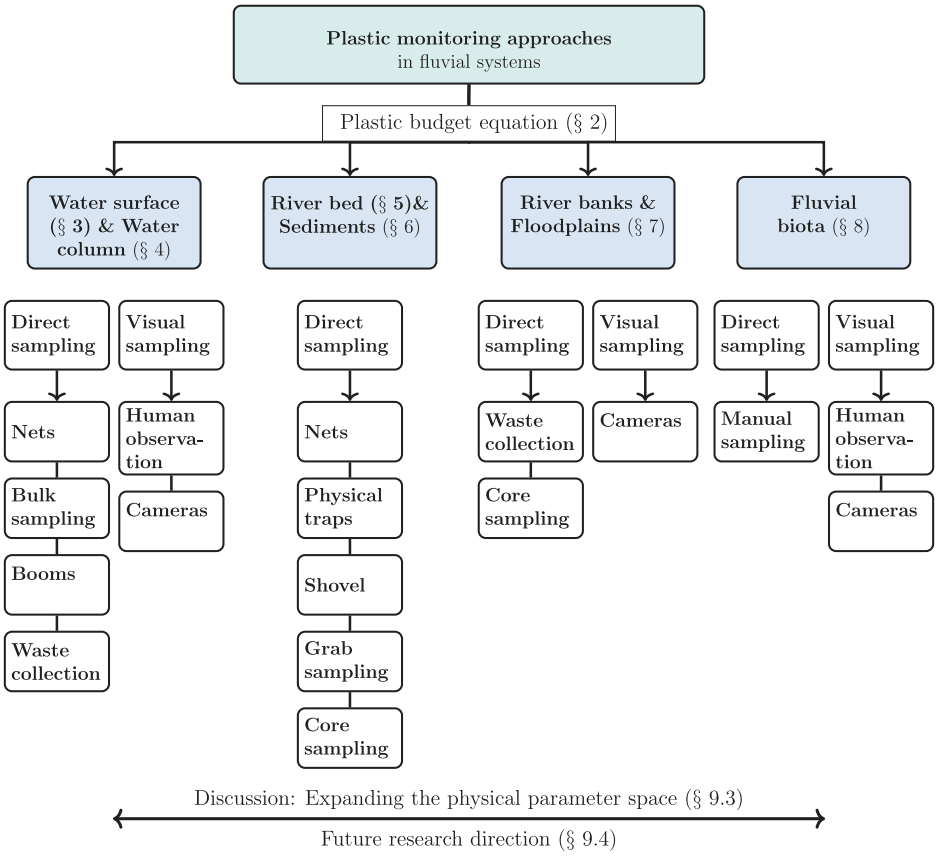

Fig. 1. Current monitoring strategies for fluvial plastics.

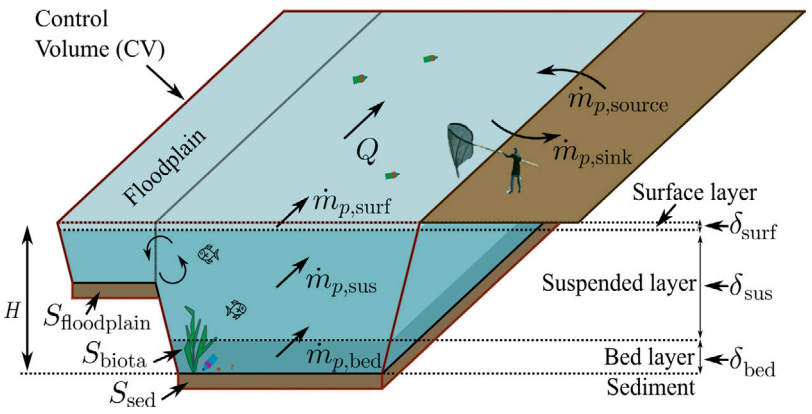

Fig. 2. Control volume approach used to define the plastic budget equation for a simplified river section, including transport layers and storage compartments; control volume CV indicated with red border; $\dot{m}_p$ = plastic mass flow rate; S = plastic store; H = water depth; Q = water flow rate; δ = water layer thickness.

2. Plastic budget equation

To quantify the movement of plastics, we turn to the formulation of the plastic budget equation for fluvial systems, which write for plastics using a control volume approach, further invoking the Reynolds transport theorem (Kundu et al., 2012)

$$\frac{\mathrm{d}m_{p,\text{sys}}}{\mathrm{d}t} = \underbrace{\frac{\mathrm{d}}{\mathrm{d}t}\iiint_{\text{CV}} c_p \,\mathrm{d}\mathcal{V}}_{\substack{\text{change of plastic}\\ \text{mass within CV}}} + \underbrace{\iint_{\text{CS}} c_p \mathbf{v}\cdot\hat{\mathbf{n}}\,\mathrm{d}A}_{\substack{\text{plastic mass flow}\\ \text{through CS}}}, \tag{1}$$

where $\mathrm{d}m_{p,\text{sys}}/\mathrm{d}t$ is the rate of change of plastic mass in the system, c_p is the plastic concentration, $\mathrm{d}\mathcal{V}$ is an infinitesimal volume of the control volume CV, $\mathbf{v}$ is the fluid velocity vector, $\mathrm{d}A$ is an infinitesimal area of the control surface CS, and $\hat{\mathbf{n}}$ is the normal vector perpendicular to $\mathrm{d}A$. We simplify the rate of change of plastic mass within the control volume as

$$\frac{\mathrm{d}}{\mathrm{d}t}\iiint_{\text{CV}} c_p \,d\mathcal{V} = \frac{\mathrm{d}S}{\mathrm{d}t}, \tag{2}$$

where S is a storage term. Eqs. (1) and (2) are now applied to the control volume shown in Fig. 2, which is conceptualized to span between two monitoring stations. We note that the CV can be arbitrarily defined, however, it is advantageous to select the control volume such that the boundaries are well defined, implying that mass fluxes are normal to the boundaries, and that flow properties are known; multiple control volumes may be defined along a river stretch. Using plastic mass conservation, i.e., $\mathrm{d}m_{p,\text{sys}}/\mathrm{d}t = 0$, substituting this into Eq. (1), and using Eq. (2), we obtain

$$\frac{\mathrm{d}S}{\mathrm{d}t} = -\iint_{\text{CS}} c_p \mathbf{v}\cdot\hat{\mathbf{n}}\,\mathrm{d}A. \tag{3}$$

Next, we distinguish different storage compartments within our CV, comprising surface layer, suspended layer, and bed layer, as well as storage in sediments, floodplains (including river banks), and biota (Fig. 2), therefore Eq. (3) can be re-written as

$$\frac{\mathrm{d}S_{\text{surf}}}{\mathrm{d}t} + \frac{\mathrm{d}S_{\text{sus}}}{\mathrm{d}t} + \frac{\mathrm{d}S_{\text{bed}}}{\mathrm{d}t} + \frac{\mathrm{d}S_{\text{sed}}}{\mathrm{d}t} + \frac{\mathrm{d}S_{\text{floodplain}}}{\mathrm{d}t} + \frac{\mathrm{d}S_{\text{biota}}}{\mathrm{d}t} = -\iint_{\text{CS}} c_p \mathbf{v}\cdot\hat{\mathbf{n}}\,\mathrm{d}A, \tag{4}$$

where the terms on the left-hand side represent the rates of change of plastic mass stored in various compartments within the river system, including water surface (S_{surf}), suspended layer (S_{sus}), riverbed (S_{bed}), bed sediments (S_{sed}), floodplains ($S_{\text{floodplain}}$), and biota ($\mathrm{d}S_{\text{biota}}$), c.f. Fig. 2. In this formulation, the budget equation is written for the total plastic mass present in the control volume, independent of particle size. By inspecting Eq. (4), it is obvious that the changes of stored plastic mass in the surface layer, suspended layer, and bed layer, which are predominantly transport layers, are much smaller than the accumulation in sediments, river banks, floodplains, and biota, thus we can simplify

$$\frac{\mathrm{d}S_{\text{sed}}}{\mathrm{d}t} + \frac{\mathrm{d}S_{\text{floodplain}}}{\mathrm{d}t} + \frac{\mathrm{d}S_{\text{biota}}}{\mathrm{d}t} = \sum \dot{m}_{p,\text{in}} - \sum \dot{m}_{p,\text{out}}, \tag{5}$$

where the plastic mass flows entering and leaving the CV are explicitly written as $\dot{m}_{p,\text{in}}$ and $\dot{m}_{p,\text{out}}$. The plastic mass flows across the CS can further be associated with different physical transport modes, and it is therefore meaningful to distinguish between surface load transport, suspended load transport, and bed load transport, as well as localized source and sinks terms

$$\begin{aligned}\frac{\mathrm{d}S_{\text{sed}}}{\mathrm{d}t} + \frac{\mathrm{d}S_{\text{floodplain}}}{\mathrm{d}t} + \frac{\mathrm{d}S_{\text{biota}}}{\mathrm{d}t} = {} & \dot{m}_{p,\text{surf,in}} + \dot{m}_{p,\text{sus,in}} + \dot{m}_{p,\text{bed,in}} + \dot{m}_{p,\text{source}} \\ & - \dot{m}_{p,\text{surf,out}} - \dot{m}_{p,\text{sus,out}} - \dot{m}_{p,\text{bed,out}} - \dot{m}_{p,\text{sink}},\end{aligned} \tag{6}$$

where the indices "surf", "sus", "bed", "source", and "sink" represent mass inflows ("in") and outflows ("out") through the control surfaces of the surface layer, suspended layer, and the bed layer, as well as localized sources and sinks. The transport layers are characterized by their respective thicknesses, including the surface layer thickness δ_{surf}, the suspended layer thickness δ_{sus}, and the bed layer thickness δ_{bed} (Fig. 2); note that δ_{surf} and δ_{bed} are typically related to a plastic particle length scale, such as the particle diameter (Einstein, 1950) or the maximum diagonal length (Lofty et al., 2024), while the suspended layer thickness can simply be written $\delta_{\text{sus}} = H - \delta_{\text{surf}} - \delta_{\text{bed}}$, with H being the water depth. Eq. (6) presents a relatively simple plastic budget equation, however, an exact quantification of the individual storage and transport terms is challenging, due to the accessibility of the different compartments and layers.

In Section 3 to Section 8, we present advances in plastic monitoring to date, which allow to quantify plastic mass flows at the water surface ($\dot{m}_{p,\text{surf}}$), within the water column ($\dot{m}_{p,\text{sus}}$), and within the bed layer ($\dot{m}_{p,\text{bed}}$), as well as plastic storage in sediments (S_{sed}), floodplains and river banks ($S_{\text{floodplain}}$), and fluvial biota (S_{biota}). It is noted that some transport/storage terms are easier to measure than others, due to accessibility, and that the plastic budget equation can be resolved for one unknown term, given that the others have been determined. While solving for the source term ($\dot{m}_{p,\text{source}}$) in the plastic budget equation could provide useful insights, it is not the objective of this study. We also introduce the sink term ($\dot{m}_{p,\text{sink}}$) to represent unmonitored or untracked clean-up activities, as well as potential losses due to fragmentation into undetectable size classes (e.g., nanoplastics). Due to the uncertainties associated with both external source and sink terms, this paper does not attempt to address them.

3. Water surface

Let us revisit the measurement of floating plastic at the water surface, which include common debris such as packaging, containers, styrofoam, toys, cigarette items, clothing, and fishing gear (Van Emmerik et al., 2018). The plastic mass flow $\dot{m}_{p,\mathrm{surf}}$ entering or leaving the surface layer (Fig. 2) can be expressed through the line integral and the Reynolds decomposition $c_{p,\mathrm{surf}} = \overline{c}_{p,\mathrm{surf}} + c'_{p,\mathrm{surf}}$, $u_{\mathrm{surf}} = \overline{u}_{\mathrm{surf}} + u'_{\mathrm{surf}}$, as

$$\dot{m}_{p,\mathrm{surf}} = \int_{\mathrm{CL}} \overline{c}_{p,\mathrm{surf}}\,\overline{u}_{\mathrm{surf}}\,dy + \int_{\mathrm{CL}} \overline{c}_{p,\mathrm{surf}}\,u'_{\mathrm{surf}}\,dy + \int_{\mathrm{CL}} c'_{p,\mathrm{surf}}\,\overline{u}_{\mathrm{surf}}\,dy + \int_{\mathrm{CL}} c'_{p,\mathrm{surf}}\,u'_{\mathrm{surf}}\,dy \tag{7}$$

where CL is a control line, L is the line length, $\overline{c}_{p,\mathrm{surf}}$ is the time-averaged plastic surface concentration, $\overline{u}_{\mathrm{surf}}$ is the time-averaged surface velocity, and $c'_{p,\mathrm{surf}}$ and u'_{surf} represent turbulent fluctuations around their respective means. In the present study, we assume that these turbulent contributions are negligible compared to the mean transport and are therefore omitted from further analysis. We note that this simplification follows from the commonly adopted assumption of uniform distribution. Although plastic transport can be highly intermittent in reality, addressing the fluctuation terms remains an open challenge for future studies. Under this assumption, the plastic mass flow equation simplifies to

$$\dot{m}_{p,\mathrm{surf}} = \int_{\mathrm{CL}} \overline{c}_{p,\mathrm{surf}}\,\overline{u}_{\mathrm{surf}}\,\mathrm{d}L = \int_{y=0}^{\mathcal{B}} \overline{c}_{p,\mathrm{surf}}\,\overline{u}_{\mathrm{surf}}\,\mathrm{d}y = \alpha_{\mathrm{surf}}\,\langle \overline{c}_{p,\mathrm{surf}} \rangle\,\langle \overline{u}_{\mathrm{surf}} \rangle\,\mathcal{B}, \tag{8}$$

where $\mathcal{B}$ is the width of the cross section, and y is the transverse coordinate. Note that it was assumed that the surface velocity is perpendicular to the line L, and the latter was subsequently replaced with the width of the cross section $\mathcal{B}$. Further, the surface concentration $\langle \overline{c}_{p,\mathrm{surf}} \rangle$ and surface velocity $\langle \overline{u}_{\mathrm{surf}} \rangle$ are mean values, averaged over the width of the cross-section. Therefore the correction factor α_{surf} is introduced to account for non-uniform distributions of concentration and surface velocity across the width

$$\alpha_{\mathrm{surf}} = \frac{1}{\langle \overline{c}_{p,\mathrm{surf}} \rangle\,\langle \overline{u}_{\mathrm{surf}} \rangle\,\mathcal{B}} \int_0^{\mathcal{B}} \overline{c}_{p,\mathrm{surf}}\,\overline{u}_{\mathrm{surf}}\,\mathrm{d}y \tag{9}$$

To obtain the plastic mass flow from the surface layer in practice, a range of measurement techniques can be applied. These methods generally fall into two categories: direct sampling, which involves physically intercepting plastics at the water surface, and visual sampling, which relies on human observation or imaging technologies.

3.1. Direct sampling

Direct sampling methods (Fig. 1) involve the physical interception of floating plastics using nets (Van Emmerik et al., 2018; Geraeds et al., 2019; Van Emmerik et al., 2019a; Van Calcar and Van Emmerik, 2019; Lenaker et al., 2019), booms (Gasperi et al., 2014; Rocamora et al., 2021), bulk water samples (Wang et al., 2017; Weideman et al., 2020; Lahens et al., 2018; Barrows et al., 2017), and manual waste collection, where the litter is sampled as part of clean-up actions (Lahens et al., 2018; Bauer-Civiello et al., 2019). In the context of direct surface sampling, the surface concentration can be expressed as

$$\overline{c}_{p,\mathrm{surf}} = \frac{\sum_{i=1}^{N} m_{p,i}}{\overline{u}_{\mathrm{surf}}\,\mathcal{B}\,\mathcal{T}}, \tag{10}$$

where $m_{p,i}$ is the mass of an individual plastic item, i is a running index, and N is the total number of plastics detected during the time interval $\mathcal{T}$. It is also evident that $\dot{m}_{p,\mathrm{surf}} = \sum_{i=1}^{N} m_{p,i}/\mathcal{T}$, and that a surface flux can be defined as $\dot{m}_{p,\mathrm{surf}}/\mathcal{B} = \overline{c}_{p,\mathrm{surf}}\,\overline{u}_{\mathrm{surf}}$. We note that direct sampling methods provide direct access to most of the physical plastic parameters described in Section 1.1, specifically the evaluation of the surface concentration as per Eq. (10) is straightforward.

Nets are particularly effective for capturing microplastics, mesoplastics, and macroplastics, with mesh sizes ranging from 300 μm (Weideman et al., 2020) to 30,000 μm (Van Emmerik et al., 2018). It is worth noting that most studies have used nets exclusively, as they can provide a complete concentration profile of plastics, including surface and water column. However, their labor-intensive deployment and lack of standardization across studies reduces their efficiency for large-scale or continuous monitoring (Hurley et al., 2023). On the other hand, bulk water sampling is commonly employed to target microplastics by filtering collected water samples (Kershaw et al., 2019). This method effectively quantifies microplastic concentrations in surface and suspended layers, but yields only intermittent, point measurements, making it less suitable for capturing dynamic changes in plastic distribution.

In contrast, booms and waste collection primarily serve as mitigation strategies, but can also contribute valuable data for plastic pollution assessment. Booms are floating barriers designed to intercept buoyant debris, often deployed for large-scale clean-up efforts. While these systems are effective at isolating debris and preventing its further transport within rivers, plastics collected through booms often constitute only a small fraction, around 5% of the total collected material. The majority of the debris consists of organic matter and natural detritus, which highlights the challenge of targeting plastics specifically while managing large volumes of non-plastic materials (Gasperi et al., 2014; Rocamora et al., 2021). Importantly, booms act solely as barriers and cannot provide concentration profiles of plastics throughout the water column. Similarly, manual waste collection involves collection of debris using kayaks or small boats, acting as another mitigation-oriented approach. It is simple, often involving minimal equipment and a small team (Lahens et al., 2018; Bauer-Civiello et al., 2019). However, manual waste collection is labor-intensive, limited in spatial coverage, and unsuitable for long-term or comparable monitoring efforts.

3.2. Visual sampling

Visual sampling relies on observational techniques, such as human observers or fixed camera installations, to estimate the floating plastic load. These methods do not require physical interception of debris, and their effectiveness is influenced by factors such as river characteristics, observer expertise, environmental conditions, and monitoring objectives.

The most widely used visual approach is human observation, where individuals positioned at vantage points, e.g., bridges, document visible plastic debris floating on the water surface (Fig. 3). Note that the width of the cross-section may be divided into multiple sections, to account for the field of view of individual cameras or human observers. Observers count and classify items by type or material, often reporting the transport of floating plastics in terms of items per hour (Van Emmerik et al., 2018; Schreyers et al., 2024b). This method is relatively simple, requires minimal equipment, and offers flexibility in deployment. To enhance monitoring efforts, citizen science initiatives such as CrowdWater (CrowdWater, 2024) and The Ocean Cleanup (The Ocean Cleanup, 2024) allow volunteers to report plastic pollution sightings, expanding spatial coverage and public engagement. Despite these advantages, human observation has its limitations, as it is labor-intensive, time-consuming, and subject to fatigue, as well as issues with observer bias (Rankin et al., 2020; Kuizenga et al., 2023).

To overcome these challenges and to enhance objectivity, conventional cameras have emerged as a promising automated alternative for visual sampling. These systems allow consistent monitoring over long durations and in remote or difficult-to-access river locations (van Lieshout et al., 2020a; Tharani et al., 2021; Jakovljevic et al., 2020a). Cameras capture video footage, which is later analyzed either manually or using computer vision algorithms. In automated workflows,

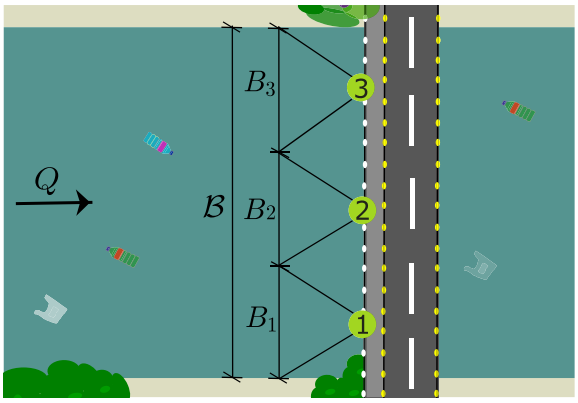

Fig. 3. Visual sampling.

tasks such as image classification, object detection, and segmentation are required to identify and quantify plastic items. In particular, object detection models are typically trained using supervised learning, where the model learns to detect and classify objects by analyzing paired input–output data. This training process allows the model to autonomously detect and potentially classify plastic debris in real-time footage. Despite their promise, camera-based systems are constrained by hardware limitations, such as battery life, file sizes, and narrow field of view, as well as strong dependency on daylight conditions (Geraeds et al., 2019). In addition, their performance can be degraded by environmental factors such as water surface glare, turbidity, wave action, and occlusion by floating organic matter.

A more advanced technological solution lies in the use of spectral cameras, which can identify materials based on their spectral signatures. These systems distinguish plastics from organic or natural debris by detecting characteristic absorption features in the near-infrared range (Goddijn-Murphy and Williamson, 2019; Tasseron et al., 2021). While laboratory studies have demonstrated their potential, field deployment remains limited due to high costs, sensitivity to illumination conditions, and dependence on controlled lighting environments (Moshtaghi et al., 2021; Goddijn-Murphy et al., 2022; Tasseron et al., 2021).

Recent advances have extended visual monitoring to satellite-based multispectral and hyperspectral remote sensing. Sentinel-2 imagery combined with machine-learning classifiers has been used to detect floating macroplastics and identify accumulation zones in riverine and coastal environments (Gómez et al., 2022; Nivedita et al., 2024), highlighting the potential of satellite remote sensing for large-scale monitoring (Marye et al., 2025). However, operational challenges remain, including limited spatial resolution for small or partially submerged items, spectral confusion with natural materials, mixed pixels at the water–land interface, atmospheric and sun-glint effects, sensitivity to turbidity and water color, and substantial computational demand. Reliable application further requires extensive ground-truth validation and site-specific calibration, currently limiting routine operational use.

We note that visual sampling methods do not provide a direct measurement of floating macroplastic mass. A common approach to overcome this limitation is the combination of a visual sampling campaign with the physical interception of a subset of floating items. From this subset, the ensemble-averaged plastic item mass $\langle \mathrm{P}_p \rangle$ is calculated as

$$\langle \mathrm{P}_p \rangle = \frac{\sum_{i=1}^{N_{\mathrm{sub}}} m_{p,i}}{N_{\mathrm{sub}}}, \tag{11}$$

where $m_{p,i}$ is the mass of the intercepted plastic item, and N_{sub} is the total number of sampled items. Once the average item mass is known, the total transported plastic mass can be estimated on the basis of the number of visually observed items

$$\sum_{i=1}^{N} m_{p,i} \approx \sum_{i=1}^{N} i \, \langle \mathrm{P}_p \rangle. \tag{12}$$

4. Water column

The distribution of plastic debris in the water column is essential for understanding its long-term persistence in aquatic environments. Suspended transport of plastics is influenced by various factors, such as plastic's submerged weight, their entrainment depth, and turbulent fluid particle interactions. In context of the plastic concentration profile, it is important to distinguish between positively buoyant ($\rho_p < \rho_w$) and negatively buoyant ($\rho_p > \rho_w$) plastics, where ρ_p is the plastic density and ρ_w the water density. Near-surface plastic transport is considerably affected by surface tension effects, and it has been shown that these effects can lead to a modification of the suspended concentration profile (Valero et al., 2022), and that the surface can act as a plastic sink (Kramer, 2025; Zaat, 2020). We summarize that positively buoyant plastics are predominantly transported in the near-surface layer, and the suspended concentration of positively buoyant plastics within the water column is $\overline{c}^{+}_{p,\mathrm{sus}} \ll \overline{c}^{+}_{p,\mathrm{surf}}$, where the superscript + is used to indicate positively buoyant plastics (Fig. 4).

The suspended concentration of negatively buoyant plastics $\overline{c}_{p,\mathrm{sus}}$ is expected to follow the well-known Rouse profile

$$\overline{c}_{p,\mathrm{sus}} = \overline{c}_{p,\mathrm{sus,ref}} \left(\frac{\frac{H}{z_{\mathrm{ref}}} - 1}{\frac{H}{z} - 1} \right)^{\beta}, \tag{13}$$

where $\overline{c}_{p,\mathrm{sus,ref}}$ is time averaged concentration of plastic at a reference height z_{ref}, H is the water depth, z is the vertical coordinate, and β is the modified Rouse number, adapted here to account for positively buoyant plastics, as first proposed by Cowger et al. (2021), defined as

$$\beta = \frac{w_t \, S_c}{\kappa \, u_\star}, \tag{14}$$

with w_t being the particle velocity, κ is the von Karman coefficient, $u_\star$ is the shear velocity, and S_c is the turbulent Schmidt number. In this definition, w_t is taken as positive when directed upward (for rising, positively buoyant particles) and negative when directed downward (for settling, negatively buoyant particles). However, Rouse-type profiles observed for suspended plastics may not be universal and remain an active area of research (Valero et al., 2022; Lofty et al., 2024), and may apply only under specific hydrodynamic conditions.

The mass of suspended plastics entering or leaving the control volume (shown in Fig. 2) can be calculated by integrating the suspended concentration over the control surface, and with Reynolds decomposition

$$\begin{aligned} \dot{m}_{p,\mathrm{sus}} = & \iint_{\mathrm{CS}} \overline{c}_{p,\mathrm{sus}} \, \overline{u} \, \mathrm{d}z \, \mathrm{d}y + \iint_{\mathrm{CS}} \overline{c}_{p,\mathrm{sus}} \, u' \, \mathrm{d}z \, \mathrm{d}y \\ & + \iint_{\mathrm{CS}} c'_{p,\mathrm{sus}} \, \overline{u} \, \mathrm{d}z \, \mathrm{d}y + \iint_{\mathrm{CS}} c'_{p,\mathrm{sus}} \, u' \, \mathrm{d}z \, \mathrm{d}y \end{aligned} \tag{15}$$

Here we neglect the contribution of the fluctuation terms to the total flux, noting that this assumption follows the same limitation discussed for the surface layer, so the suspended mass flow reduces to

$$\begin{aligned} \dot{m}_{p,\mathrm{sus}} &= \iint_{\mathrm{CS}} \overline{c}_{p,\mathrm{sus}} \, \overline{u} \, \mathrm{d}A = \int_{y=0}^{\mathcal{B}} \int_{\delta_{\mathrm{bed}}}^{H-\delta_{\mathrm{surf}}} \overline{c}_{p,\mathrm{sus}} \, \overline{u} \, \mathrm{d}z \, \mathrm{d}y \\ &= \alpha_{\mathrm{sus}} \, \langle \overline{c}_{p,\mathrm{sus}} \rangle \, \langle \overline{u} \rangle \, \mathcal{B} \, H = \alpha_{\mathrm{sus}} \, \langle \overline{c}_{p,\mathrm{sus}} \rangle \, Q \end{aligned} \tag{16}$$

where $\overline{u}$ is the time-averaged water velocity, $\mathcal{B}$ is the channel width, H is the water depth, and Q is the discharge. The correction factor α_{sus} is analogous to the α_{surf} defined for the surface layer in Section 3, accounting for non-uniform distributions of suspended plastic concentration and velocity across the section.

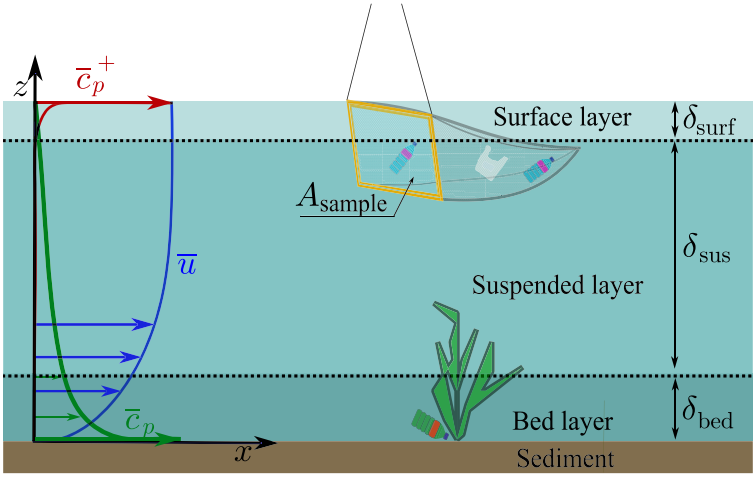

Fig. 4. Determining plastic concentrations exemplified using net sampling. $\overline{c}_p^+$ (red) - concentration of positively buoyant plastic, $\overline{c}_p$ (green) - concentration of negatively buoyant plastic.

It is also implied that the suspended plastic flux is given by $\dot{m}_{p,\mathrm{sus}}/(\mathcal{B}\,H) = \alpha_{\mathrm{sus}}\langle\overline{c}_{p,\mathrm{sus}}\rangle\,\langle\overline{u}\rangle$, and the suspended plastic concentration is typically evaluated using net sampling (Fig. 4)

$$\overline{c}_{p,\mathrm{sus}} = \frac{\sum_{i=1}^{N} m_{p,i}}{\overline{u}\,A_{\mathrm{sample}}\,\mathcal{T}}, \tag{17}$$

where m_p is the mass of an individual plastic, i is a running index, N is the total number of plastics detected during the time interval $\mathcal{T}$, and A_{sample} is the area of the net.

To capture suspended plastics of varying sizes, different types of nets are employed, with mesh sizes tailored to specific sampling interests (Lenaker et al., 2019; Tamminga et al., 2018; Haberstroh et al., 2021; Van Emmerik et al., 2019a; Abeynayaka et al., 2020). Typical sampling times range between 10 and 90 min, although Abeynayaka et al. (2020) have presented more efficient sampling systems that incorporate traditional plankton nets equipped with a waterproof propeller-powered pump to actively draw water and reduce sampling time. Previous studies revealed that fibers are the most dominant suspended microplastic type, accounting for 89% of all particles collected at subsurface depths (Lenaker et al., 2019). This is largely due to their elongated shape and the high surface area-to-volume ratio, which limits their ability to penetrate deeper in the sediment layers. As a result, they remain more exposed to water movement and are more easily resuspended by turbulence or currents (Shamskhany et al., 2021).

Another method for monitoring suspended plastics is bulk sampling, which primarily has been applied to microplastic collection at the water's surface but holds potential for targeted or depth-specific applications within the water column (Song et al., 2014). One of the limitations of this method is that it provides only point data, offering limited spatial coverage. In contrast, net-based sampling methods are typically employed to obtain concentration profiles throughout the water column. However, it is important to note that even these profiles are averaged over the net's opening area and do not offer high-resolution spatial detail.

5. River bed

Estimating plastic transport within the bed layer remains particularly challenging, as it is the least studied plastic transport layer, with scarce data and limited investigations. Only a few studies have focused on estimating plastic transport in this layer, mainly relying on net-based sampling methods (Lenaker et al., 2019; Morritt et al., 2014; Schöneich-Argent et al., 2020). Among the limited studies available, Morritt et al. (2014) stands out as the only one to have continuously deployed net sampling over three consecutive days to assess meso- and macroplastic accumulation in the bed layer. However, accurately interpreting such measurements requires a clear distinction between different plastic transport layers in the riverine environment.

To better understand plastic transport in the riverbed, it is important to distinguish between bedload and suspended load. Bedload transport refers to plastic particles that move along the riverbed through rolling, sliding, or saltation (hopping), remaining in close contact with the bottom. In contrast, suspended load consists of particles lifted into the water column by turbulence, where they remain suspended without direct contact with the bed (Van Rijn, 1984). Unlike natural sediments, where differences in size and density help clearly separate suspended particles (e.g., clay) from bedload (e.g., gravel), plastics do not follow such predictable patterns. Their wide range of shapes, densities, and surface textures means that similarly sized plastic particles can behave very differently in flow. Consequently, distinguishing between bedload and suspended plastic during sampling is not always straightforward, particularly when using net- or trap-based samplers, which may also capture particles that are settling or being resuspended.

Given the scarcity of studies on plastic transport in the bed layer, we propose leveraging measurement techniques traditionally used for sediments in this transport layer. Bedload measurement methods for sediments are typically classified into two categories: (1) direct measurement using mechanical traps, and (2) indirect measurement through remote sensing techniques, such as acoustic or optical sensors (Holmes Jr., 2010). Acoustic methods are ineffective due to the similar densities of plastics and water, which result in weak signal reflections (Chubarenko et al., 2016). Likewise, optical sensors, such as laser diffraction sensors and optical backscatter sensors, struggle with plastic detection due to the transparency and variable optical properties of plastics, complicating sensor calibration (Imhof et al., 2012). Given the current challenges with using acoustic and optical sensors to detect plastics in the bedload layer, this study focuses on direct sampling methods. Direct measurement methods for bedload, particularly mechanical trap-type samplers, are based on intercepting particles transported near the bed. Commonly used instruments for bedload sampling include the bedload transport meter Arnhem, the Helley–Smith sampler, and the Delft Nile sampler (Wiki, 2025). However, they can overestimate the transported mass due to resuspension or excess material collection and underestimate it due to gaps or blockage in the sampler opening (Wiki, 2025).

Table 2
Evaluation of sediment sampling methods by category.

Category	Sampler	Sediment type	Strengths	Limitations
Shovel	Shovel	Shallow, soft sediments	Simple, low cost	Shallow penetration
Grab	Van Veen	Soft to compact	Versatile, reliable	Shallow penetration
	Ekman	Soft, fine-grained	Light, easy to use	Not for hard beds
	Ponar	Soft to compact	Durable, adaptable	Heavy, disturbs layers
	Peterson	Compact, hard	Deep penetration	Poor for soft beds
Corer	Sediment	Stratified profiles	Preserves layers	Depth limit 10 cm
	Box	Stratified profiles	Undisturbed core	Slow, small area
	Gravity	Deeper layers	Deep sampling	Disturbs finer sediments

Building on these approaches, the transport of bedload plastics into and out of the controlled volume, as shown in Fig. 2, can be quantified by integrating their concentration over the control surface

$$\dot{m}_{p,\mathrm{bed}} = \iint_{\mathrm{CS}} \overline{c}_{p,\mathrm{bed}}\,\overline{u}\,\mathrm{d}z\,\mathrm{d}y + \iint_{\mathrm{CS}} \overline{c}_{p,\mathrm{bed}}\,u'\,\mathrm{d}z\,\mathrm{d}y + \iint_{\mathrm{CS}} c'_{p,\mathrm{bed}}\,\overline{u}\,\mathrm{d}z\,\mathrm{d}y + \iint_{\mathrm{CS}} c'_{p,\mathrm{bed}}\,u'\,\mathrm{d}z\,\mathrm{d}y. \tag{18}$$

In the present study, as discussed for the previous layers, the fluctuation terms are assumed negligible compared to the mean transport, so the bedload mass flow reduces to

$$\dot{m}_{p,\mathrm{bed}} = \iint_{\mathrm{CS}} \overline{c}_{p,\mathrm{bed}}\,\overline{u}_{\mathrm{bed}}\,\mathrm{d}A = \int_{y=0}^{\mathcal{B}}\int_{z=0}^{\delta_{\mathrm{bed}}} \overline{c}_{p,\mathrm{bed}}\,\overline{u}_{\mathrm{bed}}\,\mathrm{d}z\,\mathrm{d}y = \alpha_{\mathrm{bed}}\langle\overline{c}_{p,\mathrm{bed}}\rangle\,\langle\overline{u}_{\mathrm{bed}}\rangle\,\mathcal{B}\,H = \alpha_{\mathrm{bed}}\langle\overline{c}_{p,\mathrm{bed}}\rangle\,Q, \tag{19}$$

where $\dot{m}_{p,\mathrm{bed}}$ represents the mass flow rate of plastics in the bed layer, $\langle\overline{c}_{p,\mathrm{bed}}\rangle$ is the time and space averaged concentration of plastics in the bed layer, $\langle\overline{u}_{\mathrm{bed}}\rangle$ is the time and space averaged velocity in the bad layer, and α_{bed} is the correction factor that accounts for non-uniform distributions of plastic and velocity near the bed. Given that the commonly used methods for bedload plastic sampling involve nets and mechanical traps with rectangular profiles, the time averaged concentration of bedload plastics can be estimated as

$$\overline{c}_{p,\mathrm{bed}} = \frac{\sum_{i=1}^{N} m_{p,i}}{\overline{u}_{\mathrm{bed}}\,A_{\mathrm{sample}}\,\mathcal{T}}, \tag{20}$$

where m_p represents the mass of an individual plastic particle, i is the index for the individual plastics, N is the total number of plastics detected over a time period $\mathcal{T}$, and A_{sample} is the area of the sampling region (such as a trap or sampling device). However, due to the small span and the limited ability to sample the bed layer (δ_{bed}), it is common to combine the mass flow of suspended plastics ($\dot{m}_{p,\mathrm{sus}}$) and the bed layer ($\dot{m}_{p,\mathrm{bed}}$) plastics, typically expressing them together for the range of ($z = 0$) to ($H - \delta_{\mathrm{surf}}$), as presented in the results of Schöneich-Argent et al. (2020), Lenaker et al. (2019).

6. Sediments

Sediments serve as a repository for plastics, where they can become buried and accumulate over time. While sediments are primarily abundant with negatively buoyant plastics that sink and settle upon deposition, initially positively buoyant plastics may also eventually become buried due to biofouling accumulation of microorganisms, algae, and other organisms, which can increase their mass and alter their density, causing these plastics to sink and settle into the sediment. When it comes to sampling plastic accumulated in sediments, it is typically assessed using three main sampling techniques: shovel sampling, grab sampling, and corer sampling (Razeghi et al., 2021). The choice of method depends on the sediment type, depth, and study objectives (Table 2).

Shovel sampling is a simple and effective approach, particularly in shallow river environments where access to specialized tools is limited (Peng et al., 2018). Grab samplers are widely used for surface sediment collection, typically sampling depths up to 10 cm. The Van Veen grab is the most commonly used due to its efficiency and reliability (Gerolin et al., 2020; Duong et al., 2023; Di and Wang, 2018; Lin et al., 2018; Rodrigues et al., 2018). Other grab samplers include the Ekman grab, suited for fine-grained sediments (Firdaus et al., 2020; Vermaire et al., 2017), the Ponar grab, effective for shallow sediment layers across diverse aquatic environments (He et al., 2020), and the Peterson gravity grab, which is used for deeper sediment collection and composite sampling to minimize variability (Rao et al., 2020). On the other hand, corer samplers are preferred when undisturbed sediment profiles are needed, making them ideal for stratified sediment studies. The sediment corer is commonly used in estuarine environments for sampling depths up to 10 cm (Naidoo et al., 2015). The box corer allows for intact sediment block collection, facilitating spatial studies (Wu et al., 2020), while the gravity corer is suited for deeper sediment layers, often used to analyze microplastic distribution patterns (Fan et al., 2019).

To estimate the rate at which plastic accumulates in different storage compartment (such as sediments, floodplains, or biota), we can approximate the change in plastic mass over time using

$$\frac{\mathrm{d}S_{\mathrm{comp}}}{\mathrm{d}t} \approx \frac{\Delta S_{\mathrm{comp}}}{\Delta t} = \frac{S_{\mathrm{comp}}(t+\Delta t) - S_{\mathrm{comp}}(t)}{\Delta t}, \tag{21}$$

where, $\mathrm{d}S_{\mathrm{comp}}/\mathrm{d}t$ represents the rate of change of plastic mass within a given compartment, whether it is sediments, floodplains, or biota. ΔS_{comp} stands for the change in plastic mass within that compartment over a time interval Δt, and the accumulated plastic mass in the storage compartment, can be calculated by summing the mass of each individual plastic particle in the sample ($m_{p,i}$)

$$S_{\mathrm{comp}} = \sum_{i} m_{p,i} \tag{22}$$

The same underlying principle can be used for each storage compartment identified in Eq. (6) by simply substituting S_{comp} with the appropriate compartment-specific term, such as $S_{\mathrm{sediments}}$, $S_{\mathrm{floodplains}}$, or S_{biota}. Here, it is important to point out that the estimation of accumulated plastic in the storage compartments has focused mostly on microplastic particles, which, due to the small mass, are typically expressed as particles per kilogram of dry weight (sediment) (items kg^{-1} dw). However, this unit differs from the area-based measurements typically expressed as kilograms per square meter (kg m^{-2}), leading to discrepancies in data representation. This inconsistency highlights the need for standardizing units to ensure data comparability and facilitate the closure of plastic budgets.

7. River banks and floodplains

Floodplains and riverbanks are key storage compartments in the plastic mass equation. Recent studies underscore their importance, showing that the majority of plastics are stored within floodplains (Van Emmerik et al., 2020a; Kiessling et al., 2019). Schreyers et al. (2024c) also highlights their role as significant reservoirs of plastic

pollution, pointing out that floodplains/riverbanks account for approximately 98% of the total mass storage and between 52% to 74% of the total item storage. This discrepancy between mass and item storage percentages is expected, as plastics retained in floodplains are predominantly macroplastics, which contribute significantly to the total mass. In contrast, when considering the total number of plastic items, including microplastics, the proportion stored in floodplains appears lower. This high retention further supports our assumption from Section 2, where only floodplains, sediments, and biota are considered as storage compartments.

As Schreyers et al. (2024c) points out, the transport and retention of plastics in this storage compartment are largely influenced by lateral exchanges between the river channel and floodplains. These exchanges occur primarily through two key processes. During high-flow inundations, plastics are transported from the river channel into floodplains, where they become trapped in vegetation or accumulate within sediments. These plastics can remain stored in floodplains until they are remobilized during subsequent high-water flows. In these later events, plastics previously stored in floodplains can be reintroduced into the river channel, or moved by wind-driven forces, particularly affecting the riverbanks. While this section focuses on floodplains as storage compartments and their sampling, the hydrodynamic controls on floodplain transport during high-flow events are discussed separately in Section 9.2.

To assess plastic pollution in floodplains and riverbanks, various sampling methods are employed, that can be categorized into direct sampling and visual sampling.

7.1. Direct sampling

A physical sampling of plastic litter in this compartment involves both organized clean-up efforts and self-initiated individuals actively collecting, categorizing, and assessing macro litter (Kiessling et al., 2019; Tasseron et al., 2024; Van Emmerik et al., 2020a). A notable example is the "Plastic Pirates" project, which engages schools and youth groups in collecting and categorizing litter (Kiessling et al., 2019). While such efforts generate valuable datasets and raise awareness about plastic pollution, not all of these activities are systematically reported or sampled correctly, introducing an additional layer of uncertainty in establishing long-term trends. In contrast, microplastic pollution in this compartment has received comparatively less attention. However, Weber and Opp (2020) conducted a study using pile core driving to analyze soil samples down to a depth of 2 m. The study found that mesoplastics and microplastics were present at significantly greater depths than expected based on sedimentation rates alone, where microplastic particles have been detected between 75 and 100 cm, far deeper than the estimated 5.2 cm depth predicted by sedimentation processes. Additionally, proximity to floodplains influenced plastic accumulation, with higher concentrations detected near river channels and riparian zones, suggesting that flood events play a key role in plastic deposition and redistribution across different soil layers.

7.2. Visual sampling

Although no literature specifically addresses visual sampling methods for macroplastic litter on floodplains, we propose adapting techniques commonly used for marine shorelines to river floodplains. Aerial surveys, which have been proven effective for rapidly assessing litter distribution after natural disasters such as storms, hurricanes, or tsunamis, could be employed to evaluate floodplains following high-flow discharges. These surveys, enhanced by advancements in drone technology and artificial intelligence, could help identify litter accumulation zones, inform monitoring programs, and prioritize clean-up efforts. Similarly, fixed cameras, which have been used to monitor changes in beach morphology or litter accumulation over time, could be strategically deployed in floodplain areas to provide continuous data on litter dynamics (Kako et al., 2018).

8. Fluvial biota

Among all storage compartments, fluvial biota presents a particular challenge for quantification due to the diverse interactions between plastics, aquatic organisms, and vegetation. Estimating plastic retention in this compartment involves accounting for two primary pathways: plastics entangled in vegetation and plastic ingested by, or otherwise affecting animal life. The total plastic storage in the fluvial biotic compartment can then be expressed as shown in Section 6 through Eq. (21), yet accurately estimating it in reality remains challenging.

Many studies have confirmed microplastic ingestion in aquatic fauna, but they do not constitute systematic monitoring strategies. Microplastic ingestion is typically investigated by analyzing the digestive tracts of captured or deceased specimens to quantify ingestion rates and plastic composition. While various studies have documented microplastic ingestion across aquatic species (Murray and Cowie, 2011; Lusher et al., 2016, 2017, 2020), they primarily aim to assess which species are most affected by plastic pollution rather than to serve as a monitoring tool for plastic fluxes. While these studies are predominantly focused on microplastics, which generally represent a small portion of total plastic mass, we assume that the contribution of ingestion to overall plastic transport is minor. However, this pathway remains understudied, and its significance in the plastic budget cannot yet be fully confirmed.

Consequently, monitoring plastics in vegetation is often more straightforward than in fauna, as the entanglement of plastics in plants provides a more accessible pathway for systematic study. The estimation of plastics trapped in vegetation has only recently gained more focus (Schreyers et al., 2024a; Lotcheris et al., 2024). For instance, van Emmerik et al. (2024) employed image-based techniques to quantify water hyacinth coverage, plastic concentrations, and plastic–hyacinth aggregations along the Saigon River. They utilized bridge-mounted cameras and UAVs, combined with advanced detection computer vision algorithms. Their analysis highlighted the critical role of water hyacinths as carriers of plastics, with 81% of observed anthropogenic macrolitter found entangled within vegetation patches.

Despite the emerging interest for plastic stored in fluvial vegetation, these researches remain heavily focused on emergent vegetation, leaving submerged vegetation understudied. Visual observation, whether by human surveyors or automated camera systems, has been the primary tool for documenting plastic entanglement in emergent vegetation. However, plastics interacting with submerged plants are less visible and more challenging to quantify. Therefore, we assume that submerged vegetation likely plays a significant role in trapping plastics within aquatic environments, contributing to hidden reservoirs of contamination that are not captured in surface-focused studies.

9. Discussion

9.1. Time and length scales in the monitoring of plastics

In the previous sections, we outlined the different storage compartments and transport layers within a control volume (Fig. 2) and the corresponding approaches used to sample plastics in each. Here, we shift our focus to analyzing the time and length scales involved in plastic monitoring, as illustrated in Fig. 5.

From the reviewed literature (Table A.3), we have selected representative studies that showcase the typical size ranges of plastics sampled across various transport layers and storage compartments (Fig. 5**a**). From there, a clear trend emerges, revealing that surface sampling dominates the research landscape. However, while surface sampling is well-established, it provides only a partial view of plastic transport processes. In contrast, research about the plastic abundance in the suspended layer is noticeably less frequent. Nonetheless, existing

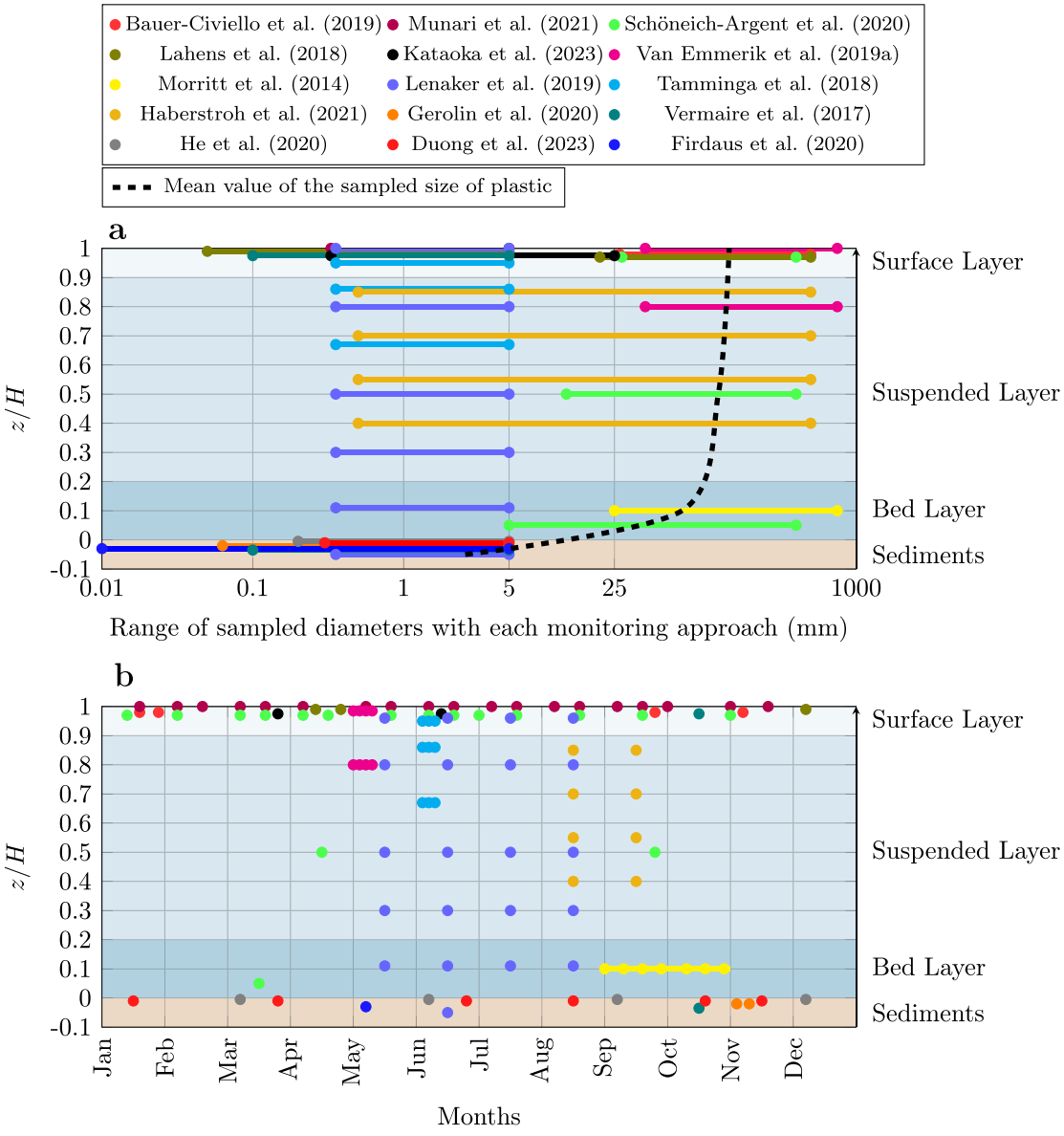

Fig. 5. Review of plastic monitoring in different layers/compartments (**a**) Length scale of sampled plastic across the water column; and (**b**) temporal distribution of sampling efforts over the course of a year.

studies demonstrate a broad range of plastic particle sizes sampled in this compartment, although no standardized sampling depths have been established. Additionally, the bed layer remains significantly understudied. While a few studies (Lenaker et al., 2019; Morritt et al., 2014; Schöneich-Argent et al., 2020) have successfully sampled plastics using net-based approaches, the scarcity of such research highlights a limited understanding of plastic dynamics in this transport layer, emphasizing the need for targeted research to bridge this gap.

The sediment compartment, on the other hand, has received relatively more attention. However, existing studies have focused predominantly on microplastics, reflecting the limitations imposed by existing sampling techniques, such as grab samplers (Firdaus et al., 2020; Vermaire et al., 2017; Gerolin et al., 2020). These methods are inherently biased toward smaller particles, leaving macroplastic dynamics in sediments largely unexplored.

Based on that, we have constructed a dashed line representing the mean value of the sampled size of plastic in each layer, which raises a fundamental question: Does the observed length scale of the measurable diameter of plastics in the water column truly represents reality, or is it merely a reflection of the limitations of current monitoring methodologies? In practice, it is likely dominated by methodological limitations, which systematically under-represent larger or denser particles, particularly in deeper or less accessible layers.

Regarding temporal scaling, Fig. 5**b** illustrates the distribution of sampling efforts across a one-year period for each of the referenced studies. Each data point represents a specific sampling instance, highlighting the frequency of monitoring across different transport layers and compartments of the water column. Similar to Fig. 5**a**, a clear pattern emerges: surface measurements are notably more frequent,

often conducted on a monthly basis (Bauer-Civiello et al., 2019; Schirinzi et al., 2020; Lahens et al., 2018; Munari et al., 2021; Lenaker et al., 2019). Some studies have extended surface monitoring over several years (Bauer-Civiello et al., 2019; Schöneich-Argent et al., 2020), while others have implemented continuous measurements over shorter periods, such as two weeks, with daily monitoring from 8:00 to 17:00 (Van Emmerik et al., 2019a; Tamminga et al., 2018). In stark contrast, sampling efforts in the deeper layers of the water column are sporadic, with research primarily concentrated between May and October. The few studies focusing on the suspended and bed layers during this period highlight the considerable challenges, both logistical and resource-related, of monitoring these compartments. For instance, in the bed layer, only Morritt et al. (2014) conducted continuous net sampling over three consecutive days, analyzing the sampled plastics afterwards. Such isolated instances underscore the limited understanding of plastic transport processes in these transport layers. This challenge is amplified when considering sediments, where the temporal scale of sampling introduces further complexity. Although sediment samples are often collected from various locations along the riverbed, these samples typically represent cumulative plastic deposition over extended periods, potentially spanning decades (10 to 30 years). This distinction raises critical questions about data interpretation: Does each sample provide a momentary snapshot of plastic deposition, or does it reflect an accumulated record of transport and burial processes over time? In most cases, sediment samples are likely to reflect long-term accumulation rather than short-term fluxes. This highlights the importance of clearly defining temporal and spatial system boundaries when interpreting storage terms in a plastic budget. Without explicit definition of the temporal and spatial window over which each compartment is assessed, mass-balance interpretations risk conflating transport and storage, thereby limiting the reliability of budget closure and trend analysis. This distinction is particularly important when interpreting unknown source and sink terms in plastic budget equations, as these terms can only be meaningfully inferred once the temporal and spatial boundaries of all transport and storage compartments are clearly defined.

9.2. Influence of hydrodynamics on plastic transport

While the preceding sections focus on how plastics are sampled across different transport layers and storage compartments, hydrodynamic conditions primarily determine when and where plastics are mobilized, transported, and stored within fluvial systems. In most natural rivers, flow conditions are predominantly turbulent, with Reynolds numbers well above the laminar–turbulent transition. These turbulent regimes enhance vertical mixing and entrainment, promoting suspended transport and downstream export of plastics, whereas lower-energy flows or transitional conditions favor deposition and local storage within the riverbed, banks, and floodplain compartments (Kumar et al., 2021).

At the upper end of this hydrodynamic spectrum, high-flow and flood events significantly alter plastic transport pathways and promote rapid redistribution across channel and floodplain compartments. Microplastics can remain mobile within inundated floodplain waters and are predominantly transported in suspension during high-discharge events, allowing them to be carried far from the main channel. As floodwaters spread across the floodplain and flow velocities decrease, microplastics are deposited together with fine sediments and organic matter in low-energy zones, leading to their incorporation into floodplain soils and mixing throughout sediment profiles (Chifflard et al., 2024). In contrast, buoyant macroplastics are mainly transported at the water surface and along floodwater margins, where deposition and storage are strongly influenced by interactions with riparian vegetation and plastic–bank interaction as water levels rise or fall. Experimental and field-based observations demonstrate that riparian vegetation density strongly controls macroplastic trapping efficiency, where large vegetation densities retain more than 90% of floating macroplastics entering the riparian zone (Valyrakis et al., 2024). Once deposited, macroplastics can remain stored on floodplain surfaces until they are remobilised during subsequent inundation events, whereas microplastics buried within floodplain sediments may persist over longer timescales but can be re-entrained during extreme flooding or erosion (Weber et al., 2022; Liro et al., 2020).

From a monitoring perspective, these hydrodynamic processes imply that representative plastic budgets cannot be derived from low-flow or snapshot measurements alone. Time-resolved observations show that a substantial proportion of annual plastic flux may occur during short-duration high-flow events, when previously stored plastics are rapidly mobilized from both the river channel and adjacent floodplains (Van Emmerik et al., 2019b; Roebroek et al., 2021; van Emmerik et al., 2023a). In extreme cases, flood-driven transport can amplify macroplastic fluxes by more than two orders of magnitude, with a large share of annual export occurring within only a few days (van Emmerik et al., 2023a). Failure to monitor these episodic fluxes therefore risks major underestimation of the annual plastic export and storage changes. However, sampling during high flows remains challenging due to elevated velocities, limited accessibility, and the instability of conventional sampling equipment, highlighting the need for monitoring strategies that explicitly target flood periods and are capable of capturing short-lived but dominant fluxes alongside longer-term baseline conditions.

9.3. Expanding the physical parameter space

Monitoring the plastic in transport layers and storage compartments in fluvial systems has heavily relied on direct or physical sampling methods. As outlined in Table 1, physical sampling methods excel in providing detailed measurements of physical parameters, which, while effective, present several challenges. These methods are often time-consuming, labor-intensive, and intermittent in their application, leading to potential gaps in data collection. The intermittent nature of physical sampling limits its capacity to capture continuous plastic transport dynamics, particularly during episodic events such as floods, which may significantly alter the plastic flow. To address these limitations, there is a growing interest in continuous monitoring techniques that can provide a more comprehensive and real-time understanding of plastic transport processes. Among all of the considerate monitoring techniques, only visual sampling using cameras stands out as a promising approach, offering a non-invasive, scalable, and potentially automated solution to complement and, in some cases, replace traditional physical sampling for some compartments.

The proposed pathway for advancing monitoring through camera-based systems is illustrated in Fig. 6. Current achievements in visual sampling focus primarily on detecting, counting, and classifying plastic, with only limited efforts dedicated to segmenting and estimating the area of pollutants. These foundational capabilities have already provided valuable insights into surface plastic transport. However, the future outlook for this approach, driven by advancements in computer vision technologies, extends to parameters such as density, mass, mass flow, trajectory tracking, and remote velocity estimation. At the highest levels of this future potential, additional complexity may be captured by incorporating turbulent fluctuation terms such as v_p' and $\dot{m}'$, which represent unresolved transport mechanisms in turbulent flows. Most importantly, the strive is to achieve these insights through continuous, long-term monitoring by integrating automated real-time analysis with extended monitoring efforts.

We believe that expanding the use of camera-based monitoring should be a key focus for future research, particularly in light of insights

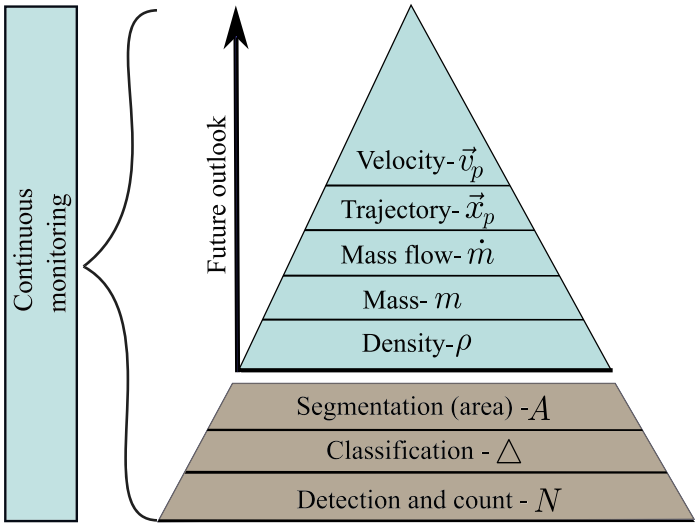

Fig. 6. Current level of achievement (brown part of the pyramid) from monitoring approaches through camera-based systems and the outlook for the future (blue).

that all positively buoyant plastics are predominantly trapped at the water's surface Fig. 4. By focusing on surface transport, camera-based systems could provide a complete assessment of positively buoyant plastics, significantly enhancing our understanding of this compartment. Furthermore, Schreyers et al. (2024c) suggests that floodplains account for up to 98% of stored plastics in river systems. This highlights another promising application of visual monitoring, combined with computer vision algorithms, that can evaluate the plastic storage across floodplain storage compartment, providing essential data for understanding long-term dynamics and designing effective mitigation strategies.

9.4. Current plastic budget equation and future aspirations

Evaluating the current plastic budget is a critical step in understanding the extent of plastic pollution in river systems. It establishes a necessary baseline for identifying key knowledge gaps and assessing the effectiveness of mitigation and remediation strategies. To systematically highlight areas requiring further investigation and technological advancements, we categorize the parameters of the plastic budget equation (Eq. (6)) into three groups: established, partially established, and unexplored (Fig. 7).

Currently, the established parameters in the plastic budget equation include the surface plastic mass flow ($\dot{m}_{p,\mathrm{surf}}$), suspended plastic mass flow ($\dot{m}_{p,\mathrm{sus}}$), and the plastic mass stored in the floodplains ($S_{\mathrm{floodplain}}$). These parameters are currently predominantly assessed through labor-intensive methods, which rely heavily on manual measurements and intermittent data collection. However, advances in particle property assessment with the integration of computer vision technologies gives the opportunity for automating this process in the future (Fig. 6), providing more reliable data for trend analysis and policy evaluation.

In addition to the established parameters, we have identified compartments and transport layers that remain inadequately explored (partially established parameters). In fact, plastics stored in sediments (S_{sed}) and bed layer ($\dot{m}_{p,\mathrm{bed}}$) have predominantly been studied for microplastic and mesoplastic, neglecting the likely substantial contributions of macroplastics. Similarly, the biota storage compartment (S_{biota}) is an overlooked area. Plastic interacting with aquatic organisms and submerged vegetation represent significant storage areas, yet they are poorly quantified. Substantial uncertainty persists across the terms of the plastic budget equation, and these uncertainties propagate through Eq. (6), particularly for compartments with sparse observations such as suspended load, bed load, and flood-driven fluxes. At present, the field lacks sufficient data for a rigorous statistical treatment of these uncertainties, and we therefore highlight this as a key research gap. Addressing these gaps will also require targeted innovation, including the development of underwater imaging systems coupled with computer-vision analysis to systematically monitor and quantify these compartments. Although these tools hold promise, further innovations will be required to fully address the complexities of these partially established parameters. We also note that micro- and nanoplastics can currently only be quantified through bulk sampling followed by laboratory analysis, which provides discrete measurements rather than continuous monitoring. As such, these size classes cannot yet be incorporated into automated or time-resolved budget assessments, so recommendations presented here apply primarily to macroplastics.

Finally, unresolved source ($\dot{m}_{p,\mathrm{source}}$) and sink ($\dot{m}_{p,\mathrm{sink}}$) terms represent the largest remaining gaps in the plastic budget equation. These terms cannot be uniquely inferred from bulk mass balances alone unless temporal and spatial system boundaries are clearly defined and additional constraints are available. Progress in constraining source terms can be achieved by increasing spatial resolution through monitoring smaller, well-defined river reaches where individual inputs dominate, by direct quantification of known emission pathways such as wastewater treatment plants, industrial discharges, and urban runoff, and by targeted event-based sampling to capture episodic releases. Sink terms may be better constrained by explicitly quantifying removal processes that are not otherwise captured in monitored compartments, including documented clean-up activities. In parallel, improved quantification of storage in retention zones can help distinguish true sinks from temporary storage. Inverse or residual-based approaches can further support source–sink estimation, but only when applied within clearly bounded systems and combined with independent measurements that reduce ambiguity between source and sink contributions.

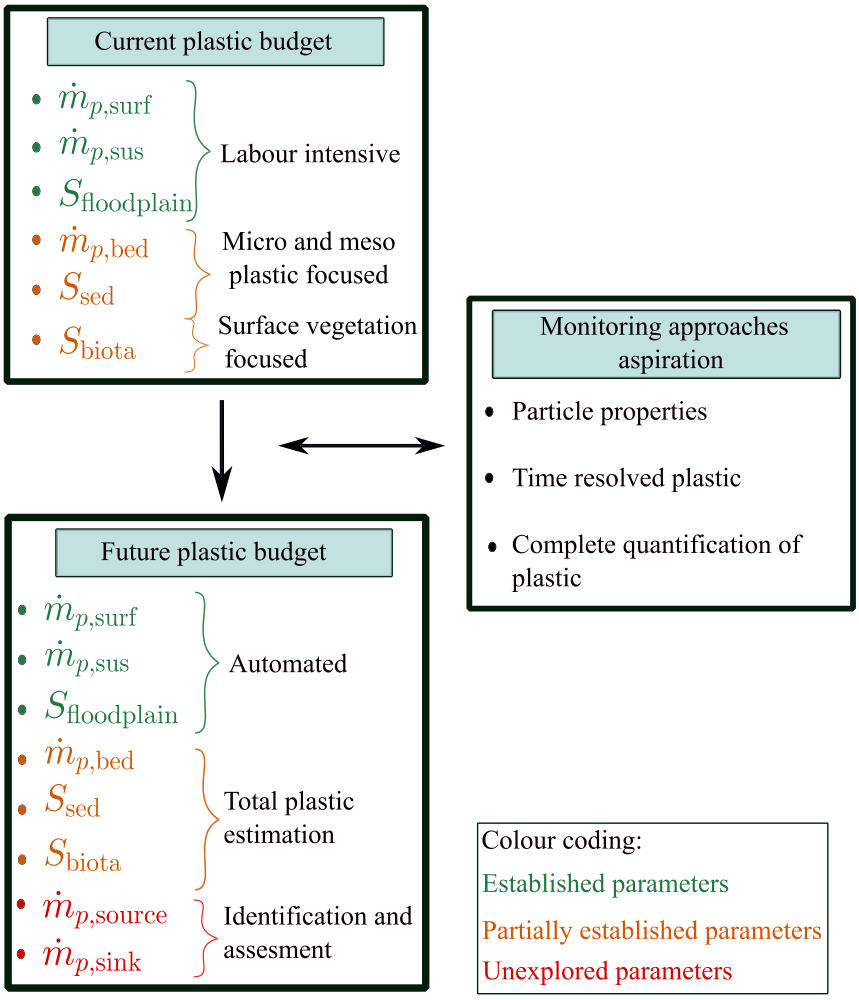

Fig. 7. Progression from the current to the future plastic budget estimation in river systems.

10. Conclusions

This review provides a comprehensive overview of current strategies for sampling plastic transport across different layers and storage compartments from the plastic budget equation. Through a structured analysis, we examine the methodologies used to quantify plastic transport and storage in riverine systems, highlighting the strengths and limitations of existing approaches.

A key takeaway from our analysis is the uneven distribution of monitoring efforts across transport layers and storage compartments. Surface plastic transport is the most extensively studied, largely due to its accessibility, while suspended and bed layer transport remains underrepresented in research. Similarly, plastic accumulation in sediments and floodplains has received more attention compared to biotic storage, which remains poorly quantified. This disparity in monitoring coverage raises concerns about the accuracy of current plastic budget estimations, emphasizing the need for a more holistic and standardized approach to data collection. Moreover, the temporal distribution of sampling efforts indicates that monitoring is often conducted sporadically and is rarely continuous, limiting our ability to capture dynamic plastic transport processes, particularly during episodic events such as floods.

To address these gaps, we advocate for expanding monitoring approaches by leveraging emerging technologies, such as camera-based systems and computer vision, to enhance plastic detection and quantification. While these advancements can improve real-time, continuous monitoring, critical knowledge gaps persist in the plastic budget equation, particularly in mass flows within the bed layer and biota, as well as the identification of plastic sources and sinks.

Nomenclature

Upper-case Roman

$\langle \mathrm{P}_p \rangle$	density of plastic items (kg/item)
$\mathcal{B}$	width of the cross section (m)
$\mathcal{T}$	time interval (s)
$\mathcal{V}$	volume (m^3)
A	area (m^2)
A_{sample}	area of the sampling instrument (m^2)
H	water depth (m)
L	line length (m)

N	number of plastic particles, (#)
N_{sub}	number of samples in the subset (#)
Q	discharge (m^3/s)
S_{bed}	storage in bed layer (kg)
S_{biota}	storage in biota (kg)
$S_{\text{floodplain}}$	storage in floodplains and river bank (kg)
S_{sed}	storage in sediments (kg)
S_{surf}	storage in surface layer (kg)
S_{sus}	storage in suspended layer(kg)
S_c	turbulent Schmidt number (–)

Lower-case Roman

α_{bed}	suspended correction factor (–)
α_{surf}	bed correction factor (–)
α_{surf}	surface correction factor (–)
β	Rouse number (–)
$\dot{m}_{p,\text{bed,in}}$	inflow of plastic mass flow in the bed compartment (kg/s)
$\dot{m}_{p,\text{bed,out}}$	outflow of plastic mass flow in the bed compartment (kg/s)
$\dot{m}_{p,\text{sink}}$	plastic mass extracted (kg/s)
$\dot{m}_{p,\text{source}}$	plastic mass from external sources (kg/s)
$\dot{m}_{p,\text{surf,in}}$	inflow of plastic mass in the surface compartment, (kg/s)
$\dot{m}_{p,\text{surf,out}}$	outflow of plastic mass in the surface compartment, (kg/s)
$\dot{m}_{p,\text{surf}}$	surface plastic mass flow, (kg/s)
$\dot{m}_{p,\text{sus,in}}$	inflow of plastic mass in the suspended compartment, (kg/s)
$\dot{m}_{p,\text{sus,out}}$	outflow of plastic mass in the suspended compartment, (kg/s)
$\dot{m}_{p,\text{sus}}$	suspended mass transport (kg/s)
$\hat{\mathbf{n}}$	normal vector,
κ	von Karman coefficient (–)
$\langle \overline{c}_{p,\text{bed}} \rangle$	spatially and time averaged bed plastic concentration (kg/m^3)
$\langle \overline{c}_{p,\text{sus}} \rangle$	spatially and time averaged concentration of plastic in suspended layer (kg/m^3)
$\langle \overline{u} \rangle$	spatially and time averaged velocity (m/s)
$\langle \overline{u}_{\text{bed}} \rangle$	spatially and time averaged velocity in bed layer (m/s)
$\mathbf{v}$	magnitude of the vector, (m/s)
$\overline{c}_{p,\text{bed}}$	time averaged concentration of plastic in bed layer (kg/m^3)
$\overline{c}_{p,\text{surf}}$	time averaged concentration of plastic in surface layer (kg/m^2)
$\overline{c}^{+}_{p,\text{surf}}$	time averaged concentration of positively buoyant surface plastics (kg/m^3)
$\overline{c}_{p,\text{sus,ref}}$	time averaged concentration of suspended plastics at reference height (kg/m^3)
$\overline{c}_{p,\text{sus}}$	time averaged concentration of plastic in suspended layer (kg/m^2)
$\overline{c}^{+}_{p,\text{sus}}$	time averaged concentration of positively buoyant suspended plastics (kg/m^3)
$\overline{u}_{\text{bed}}$	time averaged velocity in bed layer(m/s)
$\overline{u}_{\text{surf}}$	time averaged surface velocity (m/s)
$\overline{w}_t$	terminal velocity of settling plastics (m/s)
h	water depth (m)
i	running index
m_p	plastic mass (kg)
$m_{p,\text{sys}}$	plastic mass in the system (kg)
t	time (s)
$u_\star$	shear velocity (m/s)
v	flow velocity (m/s)
y	transverse coordinate
z	vertical coordinate
z_{ref}	reference height (m)
c_p	plastic concentration, (kg/m^3)

Greek letters

δ_{bed}	bed layer thickness, (m)
δ_{surf}	surface layer thickness, (m)
δ_{sus}	suspended layer thickness, (m)
λ	maximum diagonal length of a plastic particle, (m)
ρ	plastic density (kg/m^3)
$\triangle$	polymer type and shape

Abbreviations

B	river bed
CL	control line
CS	control surface
CV	control volume
FB	fluvial biota
FL	floodplains
RB	river bank
S	sediments
WC	water column
WS	water surface

CRediT authorship contribution statement

Ana Todorova: Writing – original draft, Visualization, Methodology, Investigation, Conceptualization. **Robert K. Niven:** Writing – review & editing, Supervision, Methodology, Conceptualization. **Matthias Kramer:** Writing – review & editing, Validation, Supervision, Methodology, Formal analysis, Conceptualization.

Declaration of competing interest

The authors declare that they have no known competing financial interests or personal relationships that could have appeared to influence the work reported in this paper.

Acknowledgments

The authors acknowledge the use of the AI language model ChatGPT (OpenAI) for editorial assistance. All interpretations are solely those of the authors.

Appendix. Summary of data collection

Table A.3 provides a structured overview of the reviewed literature on riverine plastic sampling. The studies are classified by transport layer (WS: water surface; WC: water column; B: river bed; S: sediment; RB: river bank; FL: floodplains; FB: fluvial biota), data-collection method, and plastic size, highlighting the diversity of observational techniques ranging from direct waste collection and net sampling to visual surveys and camera-based monitoring in both field and laboratory settings.

Data availability

No data was used for the research described in the article.

Table A.3
Summary of data collection.

No.	Reference	WS	WC	RB	S	RK	FL	FB	Properties measured	Method	Size
1	Abdel-Fattah et al. (2004)			X						physical trap	micro, meso
2	Holmes Jr. (2010)			X						physical trap	micro, meso
3	Murray and Cowie (2011)							X	N	manual sampling	micro
4	Onoi and Nihei (2012)	X							$N, \Delta, \rho, m_{p,\mathrm{surf}}$	net, camera	macro
5	Morritt et al. (2014)		X	X					$N, \Delta, \rho, m_{p,\mathrm{bed}}$	net	macro
6	Gasperi et al. (2014)	X	X						$N, \Delta, \rho, (m_{p,\mathrm{surf}} + m_{p,\mathrm{sus}})$	boom	macro
7	Naidoo et al. (2015)	X			X				N	bulk, corer	micro
8	Lusher et al. (2016)							X	N, Δ	manual sampling	micro
9	González-Fernández and Hanke (2017)	X							N, Δ	human observers	macro
10	Barrows et al. (2017)	X	X						$N, \Delta, \rho, m_{p,\mathrm{surf}}, m_{p,\mathrm{sus}}$	nets, bulk	micro
11	Vermaire et al. (2017)	X			X				N	bulk, grab	micro
12	Lusher et al. (2017)							X	N, Δ	manual sampling	micro
13	Lahens et al. (2018)	X							$N, \Delta, \rho, m_{p,\mathrm{surf}}$	bulk, manual, nets	micro, macro
14	Van Emmerik et al. (2018)	X							$N, \Delta, \rho, \dot{m}_{p,\mathrm{surf}}$	human observers, net	meso, macro
15	Zheng et al. (2018)								N, Δ, ρ	camera- lab	macro
16	Tamminga et al. (2018)	X	X						$N, \Delta, m_{p,\mathrm{surf}}$	bulk	micro
17	Kapp and Yeatman (2018)	X							$N, \Delta,$	bulk	micro
18	Di and Wang (2018)	X			X				N	bulk, grab	micro
19	Lin et al. (2018)	X			X				N	bulk, grab	micro
20	Rodrigues et al. (2018)	X			X				N	net, grab	micro
21	Kako et al. (2018)					X	X		N, Δ	camera	macro
22	Bauer-Civiello et al. (2019)	X							$N, \Delta, \rho, m_{p,\mathrm{surf}}$	manual sampling	macro
23	Geraeds et al. (2019)	X							$N, \Delta, \rho, \dot{m}_{p,\mathrm{surf}}$	human observers, camera, net	meso, macro
24	Van Emmerik et al. (2019a)	X	X						$N, \Delta, \rho, \dot{m}_{p,\mathrm{surf}}, \dot{m}_{p,\mathrm{sus}}$	human observers nets	macro
25	Van Calcar and Van Emmerik (2019)	X							$N, \Delta, \rho, \dot{m}_{p,\mathrm{surf}}$	human observers nets	meso, macro
26	Castro Jiménez et al. (2019)	X							N, Δ	human observers	macro
27	Van Emmerik et al. (2019b)	X							$\dot{N}, \Delta$	human observers	macro
28	Lenaker et al. (2019)	X	X	X	X				$N, \Delta, \rho, \dot{m}_{p,\mathrm{surf}}, \dot{m}_{p,\mathrm{sus}}, \dot{m}_{p,\mathrm{bad}}, \dot{m}_{p,\mathrm{sed}}$	nets, bulk grab	micro, meso
29	Fan et al. (2019)	X			X				N, Δ	net, corer	micro
30	Kiessling et al. (2019)					X			N, Δ	manual sampling	macro
31	Malik et al. (2020)	X	X						$N, \Delta, \rho, (m_{p,\mathrm{surf}} + m_{p,\mathrm{sus}})$	boom	meso, macro
32	Vriend et al. (2020)	X							$N, \Delta, \rho, \dot{m}_{p,\mathrm{surf}}$	human observers, boom	meso, macro
33	Schöneich-Argent et al. (2020)	X	X	X		X			$N, \Delta, \rho, \dot{m}_{p,\mathrm{surf}}, \dot{m}_{p,\mathrm{sus}}$	human observers manual, net	macro
34	Weideman et al. (2020)	X							$N, \Delta, \rho, m_{p,\mathrm{surf}}$	human observers bulk, nets	micro, meso, macro
35	van Lieshout et al. (2020b)	X							N, Δ	camera	macro
36	Jakovljevic et al. (2020b)	X							N, Δ	camera	macro
37	Kataoka and Nihei (2020)	X							N, Δ	camera	macro
38	Van Emmerik et al. (2020b)	X				X			$\dot{N}, \Delta$	human observers	macro
39	Abeynayaka et al. (2020)	X	X						$N, \Delta, \rho, \dot{m}_{p,\mathrm{sus}} \dot{m}_{p,\mathrm{surf}}$	nets	micro
40	Gerolin et al. (2020)				X				N	grab	micro
41	Firdaus et al. (2020)				X				N, Δ	grab	micro
42	He et al. (2020)				X				$N, \Delta, m_{\mathrm{sed}}$	grab	micro
43	Rao et al. (2020)				X				N, Δ	grab	micro
44	Wu et al. (2020)	X			X				N, Δ	bulk, corer	micro
45	Van Emmerik et al. (2020a)					X			N, Δ	manual sampling, corer	micro, macro
46	Weber and Opp (2020)						X		N, Δ	corer sampling	micro
47	Rocamora et al. (2021)	X	X						$N, \Delta, \rho, (m_{p,\mathrm{surf}} + m_{p,\mathrm{sus}})$	boom	macro
48	Haberstroh et al. (2021)	X	X						$N, \Delta, \rho, \dot{m}_{p,\mathrm{surf}}, \dot{m}_{p,\mathrm{sus}}$	net	micro, meso,macro
49	Munari et al. (2021)	X							N, Δ	net	meso, micro
50	Putra and Prabowo (2021)	X							N	camera	macro
51	Lin et al. (2021)	X							N, Δ, ρ	camera	macro
52	Tasseron et al. (2021)								N, Δ, ρ	camera- lab	macro
53	González-Fernández et al. (2021)								N, Δ	human observers	macro
54	Moshtaghi et al. (2021)								ρ	camera- lab	macro
55	Tharani et al. (2021)							X	N, Δ	camera	macro
56	Goddijn-Murphy et al. (2022)	X							N, Δ	camera	macro
57	Kataoka et al. (2023)	X							$N, \Delta, \rho, \dot{m}_{p,\mathrm{surf}}$	nets	micro, meso
58	van Emmerik et al. (2023b)	X				X			$N, \Delta, \rho, \dot{m}_{p,\mathrm{surf}}$	human observers, manual sampling	macro
59	Kuizenga et al. (2023)	X							$\dot{N}, \Delta$	human observers	macro
60	Pinto et al. (2023)	X						X	$\dot{N}, \Delta$	human observers	macro
61	van Emmerik et al. (2023c)	X							$\dot{N}, \Delta$	human observers	macro
62	Duong et al. (2023)				X				N, Δ	grab	micro
63	Schreyers et al. (2024b)	X							$\dot{N}, \Delta,$	human observers	macro
64	Pinto et al. (2024)	X				X			$\dot{N}, \Delta$	human observers, manual sampling	macro
65	Jia et al. (2024)	X							N, Δ	camera	macro
66	Schreyers et al. (2024a)						X		$N, \Delta, m_{p,\mathrm{floodplain}}$	manual sampling	macro
67	Lotcheris et al. (2024)							X	N, Δ	camera	macro
68	van Emmerik et al. (2024)							X	N, Δ, A	camera	macro

References

Abdel-Fattah, S., Amin, A., Van Rijn, L., 2004. Sand transport in Nile river, Egypt. J. Hydraul. Eng. 130 (6), 488–500.

Abeynayaka, A., Kojima, F., Miwa, Y., Ito, N., Nihei, Y., Fukunaga, Y., Yashima, Y., Itsubo, N., 2020. Rapid sampling of suspended and floating microplastics in challenging riverine and coastal water environments in Japan. Water 12 (7), 1903.

Andrady, A.L., 2003. Plastics and the Environment. John Wiley & Sons.

Andrady, A.L., Neal, M.A., 2009. Applications and societal benefits of plastics. Phil. Trans. R. Soc. B 364 (1526), 1977–1984.

Barnes, D.K., Galgani, F., Thompson, R.C., Barlaz, M., 2009. Accumulation and fragmentation of plastic debris in global environments. Phil. Trans. R. Soc. B 364 (1526), 1985–1998.

Barrows, A.P., Neumann, C.A., Berger, M.L., Shaw, S.D., 2017. Grab vs. neuston tow net: a microplastic sampling performance comparison and possible advances in the field. Anal. Methods 9 (9), 1446–1453.

Bauer-Civiello, A., Critchell, K., Hoogenboom, M., Hamann, M., 2019. Input of plastic debris in an urban tropical river system. Marine Poll. Bull. 144, 235–242. http://dx.doi.org/10.1016/j.marpolbul.2019.04.070.

Castro Jiménez, J., González-Fernández, D., Fornier, M., Schmidt, N., Sempéré, R., 2019. Macro-litter in surface waters from the rhone river: Plastic pollution and loading to the NW mediterranean sea. Marine Poll. Bull. 146, 60–66.

Chifflard, P., Nather, T., Weber, C.J., 2024. Transport of (micro) plastic within a river cross-section—Spatio-temporal variations and loads. Microplastics 3 (4), 755–770.

Chubarenko, I., Bagaev, A., Zobkov, M., Esiukova, E., 2016. On some physical and dynamical properties of microplastic particles in marine environment. Marine Poll. Bull. 108 (1–2), 105–112.

Cowger, W., Gray, A.B., Guilinger, J.J., Fong, B., Waldschläger, K., 2021. Concentration depth profiles of microplastic particles in river flow and implications for surface sampling. Environ. Sci. Technol. 55 (9), 6032–6041.

CrowdWater, 2024. Plastic pollution monitoring. URL https://crowdwater.ch/en/plastic-pollution/. (Accessed 25 March 2024).

Derraik, J.G., 2002. The pollution of the marine environment by plastic debris: a review. Marine Poll. Bull. 44 (9), 842–852.

Di, M., Wang, J., 2018. Microplastics in surface waters and sediments of the three gorges reservoir, China. Sci. Total Environ. 616, 1620–1627.

Duong, T.T., Nguyen-Thuy, D., Phuong, N.N., Ngo, H.M., Doan, T.O., Le, T.P.Q., Bui, H.M., Nguyen-Van, H., Nguyen-Dinh, T., Nguyen, T.A.N., et al., 2023. Microplastics in sediments from urban and suburban rivers: Influence of sediment properties. Sci. Total Environ. 904, 166330.

Einstein, H.A., 1950. The Bed-Load Function for Sediment Transportation in Open Channel Flows. (1026), US Department of Agriculture.

van Emmerik, T.H., Frings, R.M., Schreyers, L.J., Hauk, R., de Lange, S.I., Mellink, Y.A., 2023a. River plastic transport and deposition amplified by extreme flood. Nat. Water 1 (6), 514–522.

van Emmerik, T.H.M., Janssen, T.W., Jia, T., Bui, T.-K.L., Taormina, R., Nguyen, H.-Q., Schreyers, L.J., 2024. Water hyacinths as riverine plastic pollution carriers. EGUsphere 2024, 1–24.

van Emmerik, T.H., Kirschke, S., Schreyers, L.J., Nath, S., Schmidt, C., Wendt-Potthoff, K., 2023b. Estimating plastic pollution in rivers through harmonized monitoring strategies. Marine Poll. Bull. 196, http://dx.doi.org/10.1016/j.marpolbul.2023.115503.

van Emmerik, T.H., Schreyers, L.J., Mellink, Y.A., Sok, T., Arias, M.E., 2023c. Large variation in mekong river plastic transport between wet and dry season. Front. Environ. Sci. 11, 1173946.

van Emmerik, T., Schwarz, A., 2020. Plastic debris in rivers. Wiley Interdiscip. Rev.: Water 7 (1), e1398.

Fan, Y., Zheng, K., Zhu, Z., Chen, G., Peng, X., 2019. Distribution, sedimentary record, and persistence of microplastics in the Pearl River catchment, China. Environ. Pollut. 251, 862–870.

Firdaus, M., Trihadiningrum, Y., Lestari, P., 2020. Microplastic pollution in the sediment of Jagir estuary, Surabaya city, Indonesia. Marine Poll. Bull. 150, 110790.

Gall, S.C., Thompson, R.C., 2015. The impact of debris on marine life. Marine Poll. Bull. 92 (1–2), 170–179.

Gasperi, J., Dris, R., Bonin, T., Rocher, V., Tassin, B., 2014. Assessment of floating plastic debris in surface water along the Seine river. Environ. Pollut. 195, 163–166.

Geraeds, M., van Emmerik, T., de Vries, R., bin Ab Razak, M.S., 2019. Riverine plastic litter monitoring using unmanned aerial vehicles (UAVs). Remote. Sens. 11 (17), 2045.

Gerolin, C.R., Pupim, F.N., Sawakuchi, A.O., Grohmann, C.H., Labuto, G., Semensatto, D., 2020. Microplastics in sediments from Amazon rivers, Brazil. Sci. Total Environ. 749, 141604.

Geyer, R., Jambeck, J.R., Law, K.L., 2017. Production, use, and fate of all plastics ever made. Sci. Adv. 3 (7), e1700782.

Goddijn-Murphy, L., Williamson, B., 2019. On thermal infrared remote sensing of plastic pollution in natural waters. Remote Sens.-Basel 11, 2159.

Goddijn-Murphy, L., Williamson, B.J., McIlvenny, J., Corradi, P., 2022. Using a UAV thermal infrared camera for monitoring floating marine plastic litter. Remote. Sens. 14 (13), 3179.

Gómez, À.S., Scandolo, L., Eisemann, E., 2022. A learning approach for river debris detection. Int. J. Appl. Earth Obs. Geoinf. 107, 102682.

González-Fernández, D., Cózar, A., Hanke, G., Viejo, J., Morales-Caselles, C., Bakiu, R., Barceló, D., Bessa, F., Bruge, A., Cabrera, M., et al., 2021. Floating macrolitter leaked from Europe into the ocean. Nat. Sustain. 4 (6), 474–483.

González-Fernández, D., Hanke, G., 2017. Toward a harmonized approach for monitoring of riverine floating macro litter inputs to the marine environment. Front. Mar. Sci. 4, 86.

Haberstroh, C.J., Arias, M.E., Yin, Z., Sok, T., Wang, M.C., 2021. Plastic transport in a complex confluence of the Mekong river in Cambodia. Environ. Res. Lett. 16 (9), 095009.

He, B., Goonetilleke, A., Ayoko, G.A., Rintoul, L., 2020. Abundance, distribution patterns, and identification of microplastics in Brisbane River sediments, Australia. Sci. Total Environ. 700, 134467.

Holmes Jr., R.R., 2010. Measurement of bedload transport in sand-bed rivers: A look at two indirect sampling methods.

Hurley, R., Braaten, H.F.V., Nizzetto, L., Steindal, E.H., Lin, Y., Clayer, F., van Emmerik, T., Buenaventura, N.T., Eidsvoll, D.P., Økelsrud, A., Norling, M., Adam, H.N., Olsen, M., 2023. Measuring riverine macroplastic: Methods, harmonisation, and quality control. (ISSN: 18792448) http://dx.doi.org/10.1016/j.watres.2023.119902.

Imhof, H.K., Schmid, J., Niessner, R., Ivleva, N.P., Laforsch, C., 2012. A novel, highly efficient method for the separation and quantification of plastic particles in sediments of aquatic environments. Limnol. Ocean.: Methods 10 (7), 524–537.

Jakovljevic, G., Govedarica, M., Alvarez-Taboada, F., 2020a. A deep learning model for automatic plastic mapping using unmanned aerial vehicle (UAV) data. Remote. Sens. 12 (9), http://dx.doi.org/10.3390/RS12091515.

Jakovljevic, G., Govedarica, M., Alvarez-Taboada, F., 2020b. A deep learning model for automatic plastic mapping using unmanned aerial vehicle (UAV) data. Remote. Sens. 12 (9), 1515.

Jambeck, J.R., Geyer, R., Wilcox, C., Siegler, T.R., Perryman, M., Andrady, A., Narayan, R., Law, K.L., 2015. Plastic waste inputs from land into the ocean. Science 347 (6223), 768–771.

Jia, T., de Vries, R., Kapelan, Z., Van Emmerik, T.H., Taormina, R., 2024. Detecting floating litter in freshwater bodies with semi-supervised deep learning. Water Res. 266, 122405.

Kako, S., Isobe, A., Kataoka, T., Yufu, K., Sugizono, S., Plybon, C., Murphy, T.A., 2018. Sequential webcam monitoring and modeling of marine debris abundance. Marine Poll. Bull. 132, 33–43.

Kapp, K.J., Yeatman, E., 2018. Microplastic hotspots in the snake and lower Columbia rivers: A journey from the greater Yellowstone ecosystem to the Pacific ocean. Environ. Pollut. 241, 1082–1090.

Kataoka, T., Nihei, Y., 2020. Quantification of floating riverine macro-debris transport using an image processing approach. Sci. Rep. 10 (1), 2198.

Kataoka, T., Tanaka, M., Mukotaka, A., Nihei, Y., 2023. Experimental uncertainty assessment of meso-and microplastic concentrations in rivers based on net sampling. Sci. Total Environ. 870, 161942.

Kershaw, P., Turra, A., Galgani, F., et al., 2019. Guidelines for the monitoring and assessment of plastic litter and microplastics in the ocean..

Kiessling, T., Knickmeier, K., Kruse, K., Brennecke, D., Nauendorf, A., Thiel, M., 2019. Plastic pirates sample litter at rivers in Germany–riverside litter and litter sources estimated by schoolchildren. Environ. Pollut. 245, 545–557.

Kramer, M., 2025. Surface detachment and bed entrainment of fluvial plastics. arXiv:2408.03081. URL https://arxiv.org/abs/2408.03081.

Kuizenga, B., Tasseron, P.F., Wendt-Potthoff, K., van Emmerik, T.H., 2023. From source to sea: Floating macroplastic transport along the Rhine river. Front. Environ. Sci. 11, http://dx.doi.org/10.3389/fenvs.2023.1180872.

Kumar, R., Sharma, P., Verma, A., Jha, P.K., Singh, P., Gupta, P.K., Chandra, R., Prasad, P.V., 2021. Effect of physical characteristics and hydrodynamic conditions on transport and deposition of microplastics in riverine ecosystem. Water 13 (19), 2710.

Kundu, P.K., Cohen, I.M., Dowling, D.R., 2012. Fluid Mechanics, fifth ed. Academic Press.

Lahens, L., Strady, E., Kieu-Le, T.-C., Dris, R., Boukerma, K., Rinnert, E., Gasperi, J., Tassin, B., 2018. Macroplastic and microplastic contamination assessment of a tropical river (Saigon River, Vietnam) transversed by a developing megacity. Environ. Pollut. 236, 661–671.

Lenaker, P.L., Baldwin, A.K., Corsi, S.R., Mason, S.A., Reneau, P.C., Scott, J.W., 2019. Vertical distribution of microplastics in the water column and surficial sediment from the Milwaukee river basin to lake Michigan. Environ. Sci. Technol. 53 (21), 12227–12237.

van Lieshout, C., van Oeveren, K., van Emmerik, T., Postma, E., 2020a. Automated River Plastic Monitoring Using Deep Learning and Cameras. Earth Space Sci. 7 (8), http://dx.doi.org/10.1029/2019EA000960.

van Lieshout, C., van Oeveren, K., van Emmerik, T., Postma, E., 2020b. Automated river plastic monitoring using deep learning and cameras. Earth Space Sci. 7 (8), e2019EA000960.

Lin, F., Hou, T., Jin, Q., You, A., 2021. Improved YOLO based detection algorithm for floating debris in waterway. Entropy 23 (9), 1111.

Lin, L., Zuo, L.Z., Peng, J.P., Cai, L.Q., Fok, L., Yan, Y., Li, H.X., Xu, X.R., 2018. Occurrence and distribution of microplastics in an urban river: a case study in the pearl river along Guangzhou city, China. Sci. Total Environ. 644, 375–381.

Liro, M., Emmerik, T.v., Wyżga, B., Liro, J., Mikuś, P., 2020. Macroplastic storage and remobilization in rivers. Water 12 (7), 2055.

Lofty, J., Valero, D., Moreno-Rodenas, A., Belay, B.S., Wilson, C., Ouro, P., Franca, 2024. On the vertical structure of non-buoyant plastics in turbulent transport. Water Res. 254, 121306.

Lotcheris, R.A., Schreyers, L., Bui, T., Thi, K., Nguyen, H.-Q., Vermeulen, B., van Emmerik, T., 2024. Plastic does not simply flow into the sea: River transport dynamics affected by tides and floating plants. Environ. Pollut. 345, 123524.

Lusher, A., Hollman, P., Mendoza-Hill, J., 2017. Microplastics in Fisheries and Aquaculture: Status of Knowledge on Their Occurrence and Implications for Aquatic Organisms and Food Safety. FAO.

Lusher, A.L., O'Donnell, C., Officer, R., O'Connor, I., 2016. Microplastic interactions with north atlantic mesopelagic fish. ICES J. Mar. Sci. 73 (4), 1214–1225.

Lusher, A., Welden, N., Sobral, P., Cole, M., 2020. Sampling, isolating and identifying microplastics ingested by fish and invertebrates. In: Analysis of Nanoplastics and Microplastics in Food. CRC Press, pp. 119–148.

Malik, N.K.A., Manaf, L.A., Jamil, N.R., Rosli, M.H., Ash'aari, Z.H., Adhar, A.S.M., 2020. Variation of floatable litter load and its compositions captured at floating debris boom (FDB) structure. J. Mater. Cycles Waste Manag. 22, 1744–1767.

Marye, A.T., Caramiello, C., De Nardi, D., Miglino, D., Proietti, G., Saddi, K.C., Biscarini, C., Manfreda, S., Poggi, M., Tauro, F., 2025. Remote sensing for monitoring macroplastics in rivers: A review. Wiley Interdiscip. Rev.: Water 12 (2), e70020.

Morritt, D., Stefanoudis, P.V., Pearce, D., Crimmen, O.A., Clark, P.F., 2014. Plastic in the thames: a river runs through it. Marine Poll. Bull. 78 (1–2), 196–200.

Moshtaghi, M., Knaeps, E., Sterckx, S., Garaba, S., Meire, D., 2021. Spectral reflectance of marine macroplastics in the VNIR and SWIR measured in a controlled environment. Sci. Rep. 11 (1), 5436.

Munari, C., Scoponi, M., Sfriso, A.A., Sfriso, A., Aiello, J., Casoni, E., Mistri, M., 2021. Temporal variation of floatable plastic particles in the largest Italian river, the po. Marine Poll. Bull. 171, 112805.

Murray, F., Cowie, P.R., 2011. Plastic contamination in the decapod crustacean nephrops norvegicus (Linnaeus, 1758). Marine Poll. Bull. 62 (6), 1207–1217.

Museum, S., 2024. The age of plastic: From parkesine to pollution. URL https://www.sciencemuseum.org.uk/objects-and-stories/chemistry/age-plastic-parkesine-pollution.

Naidoo, T., Glassom, D., Smit, A.J., 2015. Plastic pollution in five urban estuaries of KwaZulu-natal, south Africa. Marine Poll. Bull. 101 (1), 473–480.

Nivedita, V., Begum, S.S., Aldehim, G., Alashjaee, A.M., Arasi, M.A., Sikkandar, M.Y., Jayasankar, T., Vivek, S., 2024. Plastic debris detection along coastal waters using sentinel-2 satellite data and machine learning techniques. Marine Poll. Bull. 209, 117106.

Onoi, T., Nihei, Y., 2012. A new technique for evaluating floating-litter transport using temporal variation rate of water elevation. In: Proc. of 18th IAHR-APD Congress.

Peng, G., Xu, P., Zhu, B., Bai, M., Li, D., 2018. Microplastics in freshwater river sediments in Shanghai, China: a case study of risk assessment in mega-cities. Environ. Pollut. 234, 448–456.

Pinto, R.B., Barendse, T., van Emmerik, T., van der Ploeg, M., Annor, F.O., Duah, K., Udo, J., Uijlenhoet, R., 2023. Exploring plastic transport dynamics in the Odaw river, Ghana. Front. Environ. Sci. 11, 1125541.

Pinto, R.B., Bogerd, L., van der Ploeg, M., Duah, K., Uijlenhoet, R., van Emmerik, T.H., 2024. Catchment scale assessment of macroplastic pollution in the Odaw river, Ghana. Marine Poll. Bull. 198, 115813.

Putra, F.F., Prabowo, Y.D., 2021. Low resource deep learning to detect waste intensity in the river flow. Bull. Electr. Eng. Inform. 10 (5), 2724–2732.

Rankin, S., Oedekoven, C., Archer, F., 2020. Mark recapture distance sampling: using acoustics to estimate the fraction of dolphins missed by observers during shipboard line-transect surveys. Environ. Ecol. Stat. 27 (2), 233–251.

Rao, Z., Niu, S., Zhan, N., Wang, X., Song, X., 2020. Microplastics in sediments of river yongfeng from Maanshan city, Anhui province, China. Bull. Environ. Contam. Toxicol. 104, 166–172.

Razeghi, N., Hamidian, A.H., Wu, C., Zhang, Y., Yang, M., 2021. Microplastic sampling techniques in freshwaters and sediments: a review. [erratum: December 2021, vol. 19 (6), p. 4655].

Rocamora, C., Puerto, H., Abadía, R., Brugarolas, M., Martínez-Carrasco, L., Cordero, J., 2021. Floating debris in the low segura river basin (Spain): Avoiding litter through the irrigation network. Water 13 (8), 1074.

Rodrigues, M., Abrantes, N., Gonçalves, F., Nogueira, H., Marques, J., Gonçalves, A., 2018. Spatial and temporal distribution of microplastics in water and sediments of a freshwater system (Antuã river, Portugal). Sci. Total Environ. 633, 1549–1559.

Roebroek, C.T., Harrigan, S., Van Emmerik, T.H., Baugh, C., Eilander, D., Prudhomme, C., Pappenberger, F., 2021. Plastic in global rivers: are floods making it worse? Environ. Res. Lett. 16 (2), 025003.

Schirinzi, G.F., Köck-Schulmeyer, M., Cabrera, M., González-Fernández, D., Hanke, G., Farré, M., Barceló, D., 2020. Riverine anthropogenic litter load to the mediterranean sea near the metropolitan area of Barcelona, Spain. Sci. Total Environ. 714, 136807.

Schöneich-Argent, R.I., Dau, K., Freund, H., 2020. Wasting the north sea?–a field-based assessment of anthropogenic macrolitter loads and emission rates of three German tributaries. Environ. Pollut. 263, 114367.

Schreyers, L.J., van Emmerik, T.H., Bui, T.K.L., Biermann, L., Uijlenhoet, R., Nguyen, H.Q., Wallerstein, N., van der Ploeg, M., 2024a. Water hyacinths retain river plastics. Environ. Pollut. 356, 124118.

Schreyers, L.J., van Emmerik, T.H.M., Bui, T.K.L., van Thi, K.L., Vermeulen, B., Nguyen, H.Q., Wallerstein, N., Uijlenhoet, R., van der Ploeg, M., 2024b. River plastic transport affected by tidal dynamics. Hydrol. Earth Syst. Sci. 28 (3), 589–610. http://dx.doi.org/10.5194/hess-28-589-2024, URL https://hess.copernicus.org/articles/28/589/2024/.

Schreyers, L.J., van Emmerik, T.H., Huthoff, F., Collas, F.P., Wegman, C., Vriend, P., Boon, A., de Winter, W., Oswald, S.B., Schoor, M.M., et al., 2024c. River plastic transport and storage budget. Water Res. 259, 121786.

Shamskhany, A., Li, Z., Patel, P., Karimpour, S., 2021. Evidence of microplastic size impact on mobility and transport in the marine environment: a review and synthesis of recent research. Front. Mar. Sci. 8, 760649.

Song, Y.K., Hong, S.H., Jang, M., Kang, J.H., Kwon, O.Y., Han, G.M., Shim, W.J., 2014. Large accumulation of micro-sized synthetic polymer particles in the sea surface microlayer. Environ. Sci. Technol. 48 (16), 9014–9021.

Tamminga, M., Hengstmann, E., Fischer, E.K., 2018. Microplastic analysis in the South Funen Archipelago, Baltic Sea, implementing manta trawling and bulk sampling. Marine Poll. Bull. 128, 601–608.

Tasseron, P.F., van Emmerik, T.H., de Winter, W., Vriend, P., van der Ploeg, M., 2024. Riverbank plastic distributions and how to sample them. Microplastics Nanoplastics 4 (1), 22.

Tasseron, P., Van Emmerik, T., Peller, J., Schreyers, L., Biermann, L., 2021. Advancing floating macroplastic detection from space using experimental hyperspectral imagery. Remote. Sens. 13 (12), 2335.

Tharani, M., Amin, A.W., Rasool, F., Maaz, M., Taj, M., Muhammad, A., 2021. Trash detection on water channels. In: Neural Information Processing: 28th International Conference, ICONIP 2021, Sanur, Bali, Indonesia, December 8–12, 2021, Proceedings, Part I 28. Springer, pp. 379–389.

The Ocean Cleanup, 2024. Plastic pollution sources. URL https://theoceancleanup.com/sources/. (Accessed 25 March 2024).

Valero, D., Belay, B.S., Moreno-Rodenas, A., Kramer, M., Franca, M.J., 2022. The key role of surface tension in the transport and quantification of plastic pollution in rivers. Water Res. 226, 119078.

Valyrakis, M., Gilja, G., Liu, D., Latessa, G., 2024. Transport of floating plastics through the fluvial vector: the impact of riparian zones. Water 16 (8), 1098.

Van Calcar, C., Van Emmerik, T., 2019. Abundance of plastic debris across European and Asian rivers. Environ. Res. Lett. 14 (12), 124051.

Van Emmerik, T., Kieu Le, T.C., Loozen, M., Van Oeveren, K., Strady, E., Bui, X.-T., Egger, M., Gasperi, J., Lebreton, L., Nguyen, P.D., et al., 2018. A methodology to characterize riverine macroplastic emission into the ocean. Front. Mar. Sci. 5, 372.

Van Emmerik, T., Loozen, M., Van Oeveren, K., Buschman, F., Prinsen, G., 2019a. Riverine plastic emission from Jakarta into the ocean. Environ. Res. Lett. 14 (8), 084033.

Van Emmerik, T., Roebroek, C., De Winter, W., Vriend, P., Boonstra, M., Hougee, M., 2020a. Riverbank macrolitter in the Dutch Rhine–Meuse delta. Environ. Res. Lett. 15 (10), 104087.

Van Emmerik, T., Seibert, J., Strobl, B., Etter, S., Den Oudendammer, T., Rutten, M., bin Ab Razak, M.S., van Meerveld, I., 2020b. Crowd-based observations of riverine macroplastic pollution. Front. Earth Sci. 8, 298.

Van Emmerik, T., Tramoy, R., Van Calcar, C., Alligant, S., Treilles, R., Tassin, B., Gasperi, J., 2019b. Seine plastic debris transport tenfolded during increased river discharge. Front. Mar. Sci. 6, 642.

Van Rijn, L.C., 1984. Sediment transport, part I: bed load transport. J. Hydraul. Eng. 110 (10), 1431–1456.

Vermaire, J.C., Pomeroy, C., Herczegh, S.M., Haggart, O., Murphy, M., 2017. Microplastic abundance and distribution in the open water and sediment of the Ottawa River, Canada, and its tributaries. Facets 2 (1), 301–314.

Vriend, P., Van Calcar, C., Kooi, M., Landman, H., Pikaar, R., Van Emmerik, T., 2020. Rapid assessment of floating macroplastic transport in the Rhine. Front. Mar. Sci. 7, 10.

Wang, W., Ndungu, A.W., Li, Z., Wang, J., 2017. Microplastics pollution in inland freshwaters of China: A case study in urban surface waters of Wuhan, China. Sci. Total Environ. 575, 1369–1374.

Weber, C.J., Opp, C., 2020. Spatial patterns of mesoplastics and coarse microplastics in floodplain soils as resulting from land use and fluvial processes. Environ. Pollut. 267, 115390.

Weber, C.J., Opp, C., Prume, J.A., Koch, M., Andersen, T.J., Chifflard, P., 2022. Deposition and in-situ translocation of microplastics in floodplain soils. Sci. Total Environ. 819, 152039.

Weideman, E.A., Perold, V., Ryan, P.G., 2020. Limited long-distance transport of plastic pollution by the Orange-Vaal river system, South Africa. Sci. Total Environ. 727, 138653.

Wiki, C., 2025. Measuring instruments for sediment transport: Description of bed load samplers. URL https://www.coastalwiki.org/wiki/Measuring_instruments_for_sediment_transport#Description_of_bed_load_samplers. (Accessed 22 January 2025).

Wu, P., Tang, Y., Dang, M., Wang, S., Jin, H., Liu, Y., Jing, H., Zheng, C., Yi, S., Cai, Z., 2020. Spatial-temporal distribution of microplastics in surface water and sediments of Maozhou River within Guangdong-Hong Kong-Macao Greater Bay Area. Sci. Total Environ. 717, 135187.

Zaat, L.A., 2020. Below the Surface (Ph.D. thesis, MSc thesis). Delft University of Technology, Delft, Netherlands.

Zheng, Y., Bai, J., Xu, J., Li, X., Zhang, Y., 2018. A discrimination model in waste plastics sorting using NIR hyperspectral imaging system. Waste Manage. 72, 87–98.